NANOSTRUCTURED Pt/MnO_2 CATALYSTS AND THEIR PERFORMANCE FOR OXYGEN REDUCTION REACTION IN AIR CATHODE MICROBIAL FUEL CELL

CHAN KAR MIN

BACHELOR OF CHEMICAL ENGINEERING
UNIVERSITI MALAYSIA PAHANG

Thesis Access Form

No_____Location_____

Author : ……

Title : ……

Status of access OPEN / RESTRICTED / CONFIDENTIAL

Moratorium period:_____ years, ending_____/_____200____

Conditions of access proved by (CAPITALS): DR. MD. MAKSUDUR RAHMAN KHAN

Supervisor (Signature)……

Faculty: ……

Author's Declaration: *I agree the following conditions:*

OPEN access work shall be made available (in the University and externally) and reproduced as necessary at the discretion of the University Librarian or Head of Department. It may also be copied by the British Library in microfilm or other form for supply to requesting libraries or individuals, subject to an indication of intended use for non-publishing purposes in the following form, placed on the copy and on any covering document or label.

*The statement itself shall apply to **ALL** copies:*

This copy has been supplied on the understanding that it is copyright material and that no quotation from the thesis may be published without proper acknowledgement.

Restricted/confidential work: All access and any photocopying shall be strictly subject to written permission from the University Head of Department and any external sponsor, if any.

Author's signature…….Date: ……

users declaration: for signature during any Moratorium period (Not Open work): ***I undertake to uphold the above conditions:***			
Date	Name (CAPITALS)	Signature	Address

NANOSTRUCTURED Pt/MnO_2 CATALYSTS AND THEIR PERFORMANCE FOR OXYGEN REDUCTION REACTION IN AIR CATHODE MICROBIAL FUEL CELL

CHAN KAR MIN

Thesis submitted in partial fulfilment of the requirements
for the award of the degree of
Bachelor of Chemical Engineering

Faculty of Chemical & Natural Resources Engineering
UNIVERSITI MALAYSIA PAHANG

JUNE 2014

SUPERVISOR'S DECLARATION

We hereby declare that we have checked this thesis and in our opinion, this thesis is adequate in terms of scope and quality for the award of the degree of Bachelor of Chemical Engineering.

Signature	:
Name of main supervisor	: DR. MD. MAKSUDUR RAHMAN KHAN
Position	: ASSOCIATE PROFESSOR
Date	: JUNE 2014

STUDENT'S DECLARATION

I hereby declare that the work in this thesis is my own except for quotations and summaries which have been duly acknowledged. The thesis has not been accepted for any degree and is not concurrently submitted for award of other degree.

Signature :
Name : CHAN KAR MIN
ID Number : KA 10068
Date : JUNE 2014

Dedication

To my supervisor, seniors, staffs, parents, and friends for being exceptionally supportive. The Secret - The Faith

ACKNOWLEDGEMENT

First and foremost, I would like to express my sincere gratitude to my supervisor, associate professor Dr. Md. Maksudur Rahman Khan, for his constant guidance, support, suggestion, encouragement, and knowledge shared throughout the entire execution of the project. Undoubtedly, with his greatest efforts and help, the project has gone smoothly, particularly in the implementation of experimental works. Furthermore, I am thankful to him for giving me a number of chances to broaden my horizons in attaining a wide spectrum of knowledge. It is fortunate enough to have the chances of learning uncommon software and analysis aside from visiting research center as well as exposed to the knowledge related to academic advancement.

In addition, I would also like to extend my deepest appreciation to post-graduate students who have been helping and guiding me a lot from time to time. Without their help, experimental works would not be conducted as smoothly as planned and there would be lots more difficulties to encounter. Furthermore, they never failed to share their knowledge despite having to engage in their works. It is indeed a valuable experience to be able to learn from them who are experienced.

Besides, I would like to thank my friends and family members for their continuous support. There have been precious supports and advice given during the ups and downs of the project. To me, they are very much treasured.

Last but not least, heartiest gratitude goes to every single person who has unconditionally lent me their helping hands in making this project not just merely possible, but successful. Thank you.

ABSTRACT

Microbial fuel cells (MFCs) represent a promising sustainable clean technology for simultaneous bioelectricity generation and wastewater treatment. Catalysts are significant portions of the cost of microbial fuel cell cathodes. Many materials have been tested as aqueous cathodes, but air-cathodes are needed to avoid energy demands for water aeration. The sluggish oxygen reduction reaction (ORR) rate at air cathode necessitates efficient electrocatalyst such as carbon supported platinum catalyst (Pt/C) which is very costly. Manganese oxide (MnO_2) was a representative metal oxide which has been studied as a promising alternative electrocatalyst for ORR and has been tested in air-cathode MFCs. However the single MnO_2 has poor electric conductivity and low stability. In the present work, the MnO_2 catalyst has been modified by doping Pt nanoparticle. The goal of the work was to improve the performance of the MFC with minimum Pt loading. MnO_2 and Pt nanoparticles were prepared by hydrothermal and sol gel methods, respectively. Wet impregnation method was used to synthesize Pt/MnO_2 catalyst. The catalysts were further used as cathode catalysts in air-cathode cubic MFCs, in which anaerobic sludge was inoculated as biocatalysts and palm oil mill effluent (POME) was used as the substrate in the anode chamber. The as-prepared Pt/MnO_2 was characterized comprehensively through field emission scanning electron microscope (FESEM), X-Ray diffraction (XRD), X-ray photoelectron spectroscopy (XPS), and cyclic voltammetry (CV) where its surface morphology, crystallinity, oxidation state and electrochemical activity were examined, respectively. XPS revealed Mn (IV) oxidation state and Pt (0) nanoparticle metal, indicating the presence of MnO_2 and Pt. Morphology of Pt/MnO_2 observed from FESEM shows that the doping of Pt change the urchin-like structure of MnO_2 into cocoon-like structure of Pt/MnO_2. The electrochemical active area of the Pt/MnO_2 catalysts has been increased from 276 to 617 m^2/g with the increase in Pt loading from 0.2 to 0.8 wt%. The CV results in O_2 saturated neutral Na_2SO_4 solution showed that MnO_2 and Pt/MnO_2 catalysts could catalyze ORR with different catalytic activities. MFC with Pt/MnO_2 (0.4 wt% Pt) as air cathode catalyst generates a maximum power density of 165 mW/m^3, which is higher than that of MFC with MnO_2 catalyst (95 mW/m^3). There was a slight increase in COD removal efficiency of 0.4 wt% Pt/MnO_2 (84%) compared to MnO_2 and other Pt loading catalysts. The open circuit voltage (OCV) of the MFC operated with MnO_2 cathode gradually decreased during 14 days of operation, whereas the MFC with Pt/MnO_2 cathode remained almost constant throughout the operation suggesting the higher stability of the Pt/MnO_2 catalyst. Therefore, Pt/MnO_2 with 0.4 wt% Pt successfully demonstrated as an efficient and low cost electrocatalyst for ORR in air cathode MFC with higher electrochemical activity, stability and hence enhanced performance as well as higher COD removal efficiency.

ABSTRAK

Sel-sel bahan api mikrob (MFCs) merupakan teknologi yang berpotensi untuk tujuan generasi bioelektrik dan rawatan air sisa serentak. Pemangkin adalah bahagian penting daripada kos katod sel bahan api mikrob. Banyak bahan telah diuji sebagai katod akueus, tetapi katod udara diperlukan bagi mengelakkan penggunaan tenaga untuk pengudaraan air. Kadar reaksi pengurangan oksigen (ORR) yang lembap di katod udara memerlukan pemangkin cekap seperti pemangkin platinum disokong karbon (Pt/C) yang amat mahal. Mangan oksida (MnO_2) adalah oksida logam yang telah dikaji sebagai pemangkin alternatif untuk ORR dan telah diuji dalam MFCs katod udara. Namun MnO_2 mempunyai kekonduksian elektrik yang lemah dan kestabilan yang rendah. Dalam karya ini, pemangkin MnO_2 telah diubah suai dengan menaburkan Pt nanopartikel. Matlamat kerja ini adalah untuk meningkatkan prestasi MFC dengan minimum kandungan Pt. MnO_2 dan Pt nanopartikel telah disediakan melalui kaedah hidroterma dan sol gel masing-masing. Kaedah pengisitepuan basah telah digunakan untuk mensintesis pemangkin Pt/MnO_2. Pemangkin digunakan sebagai pemangkin katod di katod udara MFCs padu, di mana enapcemar anaerobik telah disuntik sebagai pemangkin biologi dan bahan buangan kilang minyak sawit (POME) sebagai substrat dalam kebuk anod. Pt/MnO_2 yang disediakan dicirikan secara komprehensif melalui bidang pelepasan mikroskop imbasan elektron (FESEM), X-Ray pembelauan (XRD), sinar-X fotoelektron spektroskopi (XPS), dan voltammetri berkitar (CV) di mana morfologi permukaannya, penghabluran, pengoksidaan dan aktiviti elektrokimia telah diperiksa, masing-masing. XPS mendedahkan Mn (IV) pengoksidaan dan Pt (0) nanopartikel logam, menunjukkan kewujupan MnO_2 dan Pt. Morfologi Pt/MnO_2 yang diperhatikan dari FESEM menunjukkan bahawa penaburan Pt menyebabkan perubahan struktur urchin MnO_2 kepada struktur cocoon Pt/MnO_2. Kawasan aktif elektrokimia pemangkin Pt/MnO_2 telah meningkat dari 276 kepada 617 m^2/g dengan peningkatan dalam kandungan Pt 0.2-0.8 wt%. Peningkatan dalam keberkesanan peningkiran COD diperhatikan pada 0.4 wt% Pt/MnO_2. Keputusan CV menggunakan larutan neutral Na_2SO_4 tepu dengan O_2 menunjukkan pemangkin MnO_2 dan Pt/MnO_2 boleh menjadi pemangkin ORR dengan aktiviti-aktiviti pemangkin yang berbeza. MFC dengan Pt/MnO_2 (0.4 wt% Pt) sebagai pemangkin katod udara menjana ketumpatan kuasa maksimum 165 mW/m^3, iaitu lebih tinggi daripada MFC dengan MnO_2 pemangkin (95 mW/m^3). Voltan litar terbuka (OCV) daripada MFC dikendalikan dengan MnO_2 katod menurun secara beransur-ansur dalam 14 hari beroperasi, manakala MFC dengan Pt/MnO_2 katod yang kekal hampir malar sepanjang operasi itu mencadangkan kestabilan yang lebih tinggi oleh pemangkin Pt/MnO_2. Oleh itu, Pt/MnO_2 dengan 0.4 wt% Pt berjaya menunjukkan ia sebagai pemangkin cekap yang berkos rendah untuk ORR di katod udara MFC dengan aktiviti elektrokimia dan kestabilan yang lebih tinggi, justeru prestasi yang dipertingkatkan serta peningkiran COD yang lebih tinggi.

TABLE OF CONTENTS

LIST OF FIGURES

LIST OF TABLES

LIST OF ABBREVIATIONS

I	current
V	voltage
P	power
R	resistance
V	volume

Greek

Ω	ohm (resistance)

LIST OF ABBREVIATIONS

BET	Brunauer-Emmett-Teller
COD	Chemical oxygen demand
CV	Cyclic voltammetry
DI	Deionised water
EIS	Electrochemical impedance spectroscopy
FESEM	Field emission scanning electron microscope
MEA	Membrane electrode assembly
MFC	Microbial fuel cell
ORR	Oxygen reduction reaction
PACF	Polyacrylonitrile carbon felt
PEM	Proton exchange membrane
POME	Palm oil mill effluent
TEM	Transmission electron microscopy
XPS	X-ray photoelectron spectroscopy
XRD	X-ray diffraction

1 INTRODUCTION

1.1 Chapter Overview

In this chapter of introduction, background of study, problem statement and motivation, objective, scopes of study as well as significance of work will be presented.

1.2 Background

The major global concerns of present time are energy crisis and wastewater treatment which have triggered growing awareness. For decades, there has been heavy dependence on fossil fuels of finite supply for energy harvesting purpose. Natural gas, crude oil, and coal, for instance, are being exploited in large extent in order to meet the global massive energy demand. Undoubtedly, due to rapid advancement in civilization, energy demand of mammoth capacity is constantly on the rise. Global energy demand is expected to project to 27 TW by 2050 and 43 TW by 2100 (Lewis and Nocera, 2006). According to US Energy Information Administration (2010), the total world energy demand is around 510 quadrillion BTUs, of which approximately 450 quadrillion BTUs (88%) of world energy is derived from depleting fossil fuels which are on the brink of exhaustion. It has been estimated that the current reservoir of fossil fuels can last for another 104 years if the world consumption of renewable energy sources remains constant (US Department of Energy, 2011). There is a sheer of nearly 7% of energy needs is supplied from renewable energy resources such as solar energy, wind and hydroelectric power. Furthermore, nuclear energy, a controversial and non-renewable energy resource provides only around 5% of the world's energy supplies (Energy Information Administration, 2010). Due to public pressure and relative dangers associated with harvesting energy from atom, nuclear energy is not likely to be a major source of world energy consumption. Practically, nearly all the existing conventional energy generation technologies which require combustion of fossil fuels are cost ineffective and non-environmental friendly because of the emission of carbon dioxide (CO_2). Concentration of greenhouse gas, CO_2 is estimated will reach from 540 to 970ppmv by 2100 (Logan, 2008). This will certainly exacerbate environmental damage besides accelerate global climate change. On the account of fossil fuels' unsustainability

and polluting nature, there is an urgent and indispensable need for the searching of viable alternatives as the sustainable new renewable energy resources to resolve the critical twins problems.

Moreover, in line with the rapid development of country has inevitably contributed to the generation of huge amount of wastewater from a variety of industries. Substantial amount of energy is needed for the implementation of conventional wastewater treatment technologies. This can be exemplified in United States where an estimated 1.5% of the total electricity produced is utilized for wastewater treatment solely, and approximately 4-5% of the electrical energy is used for the whole water infrastructures (Logan, 2008). The high energy requirement has been the constant concern which critically needs promising alternative to resolve.

The discovery that microbial metabolism could provide energy in the form of electrical current has led to an increasing interest in the field of MFCs research (Allen and Bennetto, 1993). Microbial fuel cells (MFCs) represent a novel and sustainable promising technology for the simultaneous bioelectricity generation from biomass using bacteria and wastewater treatment (Logan, 2008). The main advantage of MFC technology is direct electricity generation from low grade substrates with net zero consumption of fossil fuels (Logan, 2008). The nature of substrate used as source of energy in the anode of MFC significantly affects the electricity production (Pant et al., 2010). A broad spectrum of substrates can be used in MFCs for the generation of electricity. Rabaey et al. (2003) demonstrated with success that the use of glucose as substrate in MFC is possible by generating power density two orders of magnitude greater. Apart from pure substrates like glucose and acetate, wastewater is one of the promising complex substrates as it contains various kinds of organic matters, including carbohydrate, protein, nitrogenous materials and minerals. Domestic and industrial wastewaters instead of pure substrates have been extensively studied well in recent years, swine wastewater, paper recycling plant waste, and starch processing wastewater, to name a few (Oh and Logan, 2005; Lu et al., 2009; Wang et al., 2009; Wen et al., 2009). Palm oil mill effluent (POME) is an organic industrial wastewater produced from oil palm processing plant.

Malaysia is the largest producer of palm oil globally with 49.5% of world production (Wu et al., 2008). In Malaysia, the abundance of oil palm processing industries has

contributed to the generation of substantial amount of POME. Around 3 tonnes of POME is generated with every tonne of crude palm oil produced (Ahmad et al., 2003). The existing POME treatment technologies such as anaerobic biological processes (Edewor, 1986), chemical coagulation and flotation (Badri, 1984; Chin et al., 1987; Ho and Chan, 1986), land disposal (Ma and Ong, 1986), simple skimming devices (Roge and Velayuthan, 1981), and aerobic (Abdul et al., 1989) are inefficient as they are highly energy intensive, aerobic treatment, in particular (Pham et al, 2006; Pant et al, 2007). High cost incurred for high energy supply. The major operating costs for wastewater treatment constitute of wastewater pumping, sludge treatment and wastewater aeration where half of the operation costs are contributed by aeration alone. In order to make it energy efficient, POME has recently been investigated as a potential substrate in MFC by Baranitharan and coworkers (2013). In their study, a two-chamber MFC was used and it was found that the low strength (low Chemical Oxygen Demand, COD) POME is preferable in order to achieve high efficiency in the MFC. In the two-chamber MFC, the catholyte is usually potassium permanganate solution ($KMnO_4$) and it requires extra space to operate.

Air cathode MFCs are a variation of MFCs where the cathode compartment is exposed to the air. Oxygen is the most ideal electron acceptor due to its cost effectiveness, high redox potential and sustainability comparing with many types of electron acceptors that can be used in MFC (Logan, 2008; Zhang et al., 2011). In the air-cathode MFC, due to the reduction of molecular oxygen (O_2) in cathode, it is the best choice for both chemical fuel cells and for MFCs, because the reduction product is clean and non-polluting water (H_2O). Oxygen reduction reaction (ORR) typically requires electrocatalyst for its sluggish rate. Hence, the type of electrocatalyst is vital in influencing the performance of MFCs (Cheng et al., 2006).

1.3 Problem Statement and Motivation

The driving forces which lead to the decision of developing nanostructured platinum doped manganese dioxide electrocatalyst (Pt/MnO_2) are attributed by several factors. Platinum is a well-known novel candidate of electrocatalyst which has demonstrated high electrocatalytic activity and stability for oxygen reduction reaction (ORR) in air cathode microbial fuel cell (MFC) (Steele and Heinzel, 2001).). For instances, platinum supported on carbon (Pt/C) is the common efficient catalyst used for ORR but its

application is limited due to high cost (Bashyam and Zelenay, 2006; Yu et al., 2007). Alternatively, efforts in the search for low cost catalysts are on the way. A large number of low cost catalysts have been investigated as alternatives without compromising its performance in air cathode MFC. These include macrocycle material (Zhao et al., 2005), metal porphyrins (HaoYu et al., 2007), iron phthalocyanine (Birry et al., 2011; Yuan et al., 2011; Yuan et al., 2010; Zhao et al., 2005), lead dioxide (Morris et al., 2007), Co/Fe/N/CNT (Deng et al., 2010), iron-chelated ethylenediaminetetraacetic acid (et al., 2011), nickel powder (Zhang et al., 2009), Co-naphthalocyanine (et al., 2007) and metal oxides (Morris et al., 2007). Unfortunately, these alternative catalysts have been proven as non-effective due to the long term instability (ter Heijne et al., 2007).

Non-noble catalyst, manganese dioxide (MnO_2) is among metal oxides which has been well studied and tested in air-cathode MFC recently (Cheng et al., 2010; Gong et al., 2007; Li et al., 2010; Roche et al., 2010; Roche and Scott, 2009; Zhang et al., 2009). MnO_2 exhibits advantages of low cost, environmental friendliness and high catalytic activity. Clauwaert et al. (2007) and Roche and Scott (2010) have investigated MnO_2 in neutral medium (pH 7) where it has been determined as efficient ORR catalyst. Zhang and coworkers have reported the use of MnO_2 in MFC where β-MnO_2/graphite was the efficient catalyst for ORR (2009). Furthermore, in the same year of 2010, Roche et al. used MnO_2 supported on carbon whereas Liu et al. employed single MnO_2 without catalyst support generated power density of 161 mW/m^2 and 772.8 mW/m^3, respectively. Despite of the fact that good performance been observed through these studies, stability issue found in MnO_2 was the hindrance to its widespread application in MFC. According to Hou et al., the single MnO_2 has intrinsically poor electrical conductivity and low stability. Moreover, due to its dense morphology, electrochemical performance of MnO_2 alone is not optimistic (2010).

With the aims of improving stability, electrochemical activity and hence improved MFC performance, doping of novel metals, such as platinum (Pt) or gold (Au) is believed to be able to improve the stability and performance of the catalysts. Doping of novel metals, such as Pt or Au nanoparticles (NPs) on supports has many advantages. These include increasing the number of surface atoms and hence active sites, consequently bringing synergistic effects between support and NPs, apart from lowering the cost ofcatalysts (Yu et al., 2012). The control of the novel metal loading is a critical issue

for electrocatalyst synthesis. Herein, in the present work, the MnO_2 catalyst has been modified by doping Pt NPs. The goal of the work was to improve the performance of the MFC using nanostructured Pt/MnO_2 with minimum Pt loading without compromising the low cost aimed.

1.4 Objective

The objective of the present work is to synthesize and characterize nanostructured platinum doped manganese dioxide (Pt/MnO_2) electrocatalyst as well as to investigate the performance of the electrocatalysts in air cathode microbial fuel cell (MFC) for the simultaneous electricity generation and treatment of palm oil mill effluent (POME).

1.5 Scope of Study

The scopes of the present work are to synthesize nanostructured platinum doped manganese dioxide (Pt/MnO_2) air cathode electrocatalyst by wet impregnation method from pre-synthesized platinum (Pt) nanoparticles (NPs) by sol gel method and pre-synthesized manganese dioxide (MnO_2) nanoparticles by hydrothermal method. Secondly, to characterize comprehensively electrocatalysts synthesized by field emission scanning electron microscope (FESEM), X-ray diffraction (XRD), X-ray photoelectron spectroscopy (XPS) and cyclic voltammetry (CV). Third, to fabricate membrane-electrode-assembly (MEA) by coating catalyst with Nafion solution onto carbon felt followed by hot pressing with pre-treated Nafion membrane. Lastly, performance of electrocatalyst in air cathode microbial fuel cell will be evaluated in terms of open circuit voltage (V), volumetric power density (W/m^3), and chemical oxygen demand (COD) removal efficiency.

1.6 Significance of Study

The implications of present work to society as well as environment are apparent. With the utilization of Pt/MnO_2 in air cathode microbial fuel cell (MFC) which will yield better performance and higher COD removal efficiency, its implementation in industrial sector, particularly in wastewater treatment plant will have a large degree of positive effect. For example, the electricity required for the treatment plant will be reduced which consequently reducing the operating cost apart from having net zero emission of greenhouse gases, CO_2 to the atmosphere by harvesting energy from MFC instead of

carbon sources such as fossil fuels which are of polluting nature. In addition to power generation, the treatment of waste water will be achieved to a certain degree with the degradation of organic and inorganic matter by microorganisms.

1.7 Organisation of Thesis

The structure of the remaining of the thesis is outlined as follow:

Chapter 2 provides a view of the related literature done on present work from a wide variety of spectrums. General descriptions on the working principle, configurations as well as advantages of microbial fuel cells are presented. Besides, parameters affecting the performance of microbial fuel cell are being discussed. In addition, a brief discussion of the mechanisms of oxygen reduction reaction and hence requirement for electrocatalysts is performed. Works from literature which lead to the development of the objective of current work also being discussed where a summary of the literature review is presented at the end of chapter.

Chapter 3 gives a detailed step-by-step description of the experimental works performed in the execution of the current work along with graphical aids. Besides, comprehensive analysis and characterization performed also been outlined.

Chapter 4 is devoted to the detailed and in-depth discussion of the results of characterization and analysis conducted. In addition, evidences as well as justification on any discrepancies or similarities supported with existing works are presented. Enlightening information and knowledge related to present work are provided as well in this chapter. Eventually, it revealed all the unknowns after the commencement of the experiment.

Chapter 5 draws together a summary of the thesis and outlines the future work which might be beneficial to the further development and improvement on current work.

2 LITERATURE REVIEW

2.1 Chapter Overview

Chapter 2 outlined the literature studies related to the present work. These include power generation by microbial fuel cells and its present status, factors affecting microbial fuel cell performance, air cathode microbial fuel cell, cathodic limitations of air cathode microbial fuel cell, ohmic losses, mass transport losses, activation overpotential, oxygen reduction reaction, platinum-based electrocatalysts, non-platinum based electrocatalysts, performance of non-platinum electrocatalysts, oxygen reduction reaction pathway on manganese oxides, limitations of manganese dioxide in air cathode microbial fuel cell, modification of manganese dioxide as well as the summary of all the literature review done.

2.2 Power Generation by Microbial Fuel Cells and Its Present Status

Fuel cell is a technology which has been employed as an alternative energy resource in field like transportation, portable power, and electric utility. By far, several types of fuel cell have already been developed and introduced for utilization. For examples, proton exchange membrane fuel cells (PEMFC), alkaline fuel cells (AFC), phosphoric acid fuel cells (PAFC), molten carbonate fuel cells (MCFC), solid oxide fuel cells (SOFC), direct formic acid fuel cells (DFAFC), direct methanol fuel cells (DMFC), and microbial fuel cells (MFCs) (Holland, 2007; Leong et al., 2013; Schroder, 2007).

Microbial fuel cells (MFCs) are one of the variations of bioelectrochemical fuel cells other than enzymatic fuel cells. It involves the conversion of chemical energy to electrical energy by exploiting biological components. It is a promising bioenergy technology whereby electrochemically active microorganisms, acting as biocatalyst is used to decompose a broad spectrum of organic and inorganic matters at anode through microbial respiration and electricity is harvested simultaneously (Rabaey and Verstraete, 2005; Allen and Bennetto, 1993). Microbial fuel cell commonly consists of an anode and a cathode, which separates by solid electrolyte bridge like proton exchange membrane or connected directly to wastewater substrate (Leong et al., 2013). During degradation process under anaerobic condition at the anode chamber of MFCs,

carbon dioxide, protons and electrons will be produced. The electrons and protons produced will migrate through electric circuit and membrane separator (if any), respectively and combine together with oxygen molecule at cathode to form water molecule. The typical reactions occurred at the anode (oxidation) and cathode (reduction) are presented in the equations as shown below (Liu, 2004).

Anode: $C_xH_yO_z + H_2O \rightarrow CO_2 + e^- + H^+$ (2-1)

Cathode: $O_2 + 4\ H^+ + 4\ e^- \rightarrow 2\ H_2O$ (2-2)

The overall reaction is the degradation of the substrate to carbon dioxide and water with a concomitant production of electricity.

The development of MFCs can be dated back to nearly 100 years ago. As reported by Potter (1911), he concluded that electric energy can be harvested from the microbial degradation of organic matters. In year 1931, Cohen confirmed the results reported by Potter and recorded a stacked bacterial fuel cell yielding voltage and current of 35 V and 0.2 mA, respectively. In addition, according to Suzuki (1976), microbes used as biocatalyst in MFCs was explored from the 1970s whereas the application of MFCs in wastewater treatment were reported in year 1991 (Habermann and Pommer, 1991). However, there was low power production and the impact of MFCs employed on treated wastewater's strength was unknown. It was then that in year 2004, Liu and coworkers discovered the link between the power generated using MFCs and wastewater treatment was forged as in their work domestic wastewater used could be treated to practical levels and at the same time generating electricity. MFCs are hence been developed providing possible chances for practical applications (Liu and Logan, 2004).

Various configurations of MFCs have been developed over the years, for instances, double chamber MFCs, single chamber MFCs, plate MFCs, stacked MFCs and tubular MFCs, with single and double chamber MFCs being the more common ones. The anode and the cathode of a double chamber MFC are placed in two distinct compartments where they are partitioned by a proton exchange membrane. On the contrary, the cathode of a single chamber MFC is directly exposed to the air, leaving the MFC with only a single anode chamber (Pandey et al., 2011). On the other hand, tubular MFCs have a cylindrical or tubular shape where the cathode is exposed to the air while the

membrane-electrode-assembly (MEA) is wrapped around a central anode chamber (Kim et al., 2009). In plate type MFCs having a flat rectangular shape, the MEA is sandwiched between two non-conductive rectangular plates where their inner surfaces etched with flow channels that allow wastewater to flow at the anode and air to flow at the cathode (Min and Logan, 2004).Whereas for stack MFCs, they are used for the purpose of scaling up by arranging them in a stack, either in series or in parallel, in order to generate higher voltage or larger current densities, respectively (Aelterman et al., 2006). Figures below depict different types of MFCs.

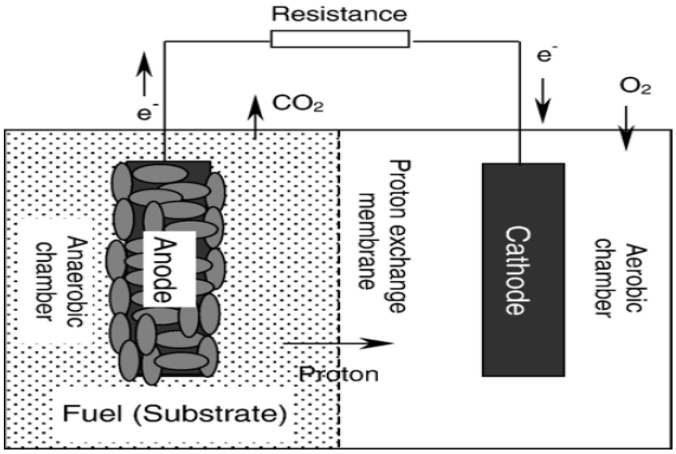

Figure 2-1:Schematic diagram of a double chamber microbial fuel cell (Du et al, 2007)

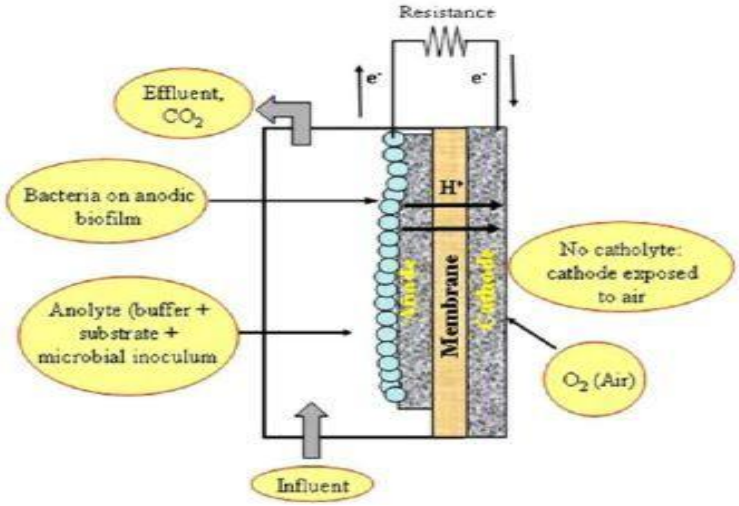

Figure 2-2: Schematic diagram of a single chamber microbial fuel cell (Du et al., 2007)

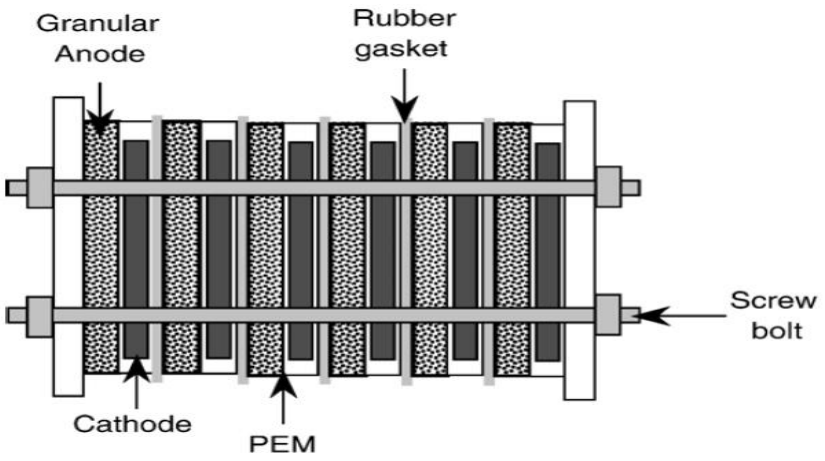

Figure 2-3: Stacked microbial fuel cells consisting of six individual units with granular graphite anode (Du et al., 2007)

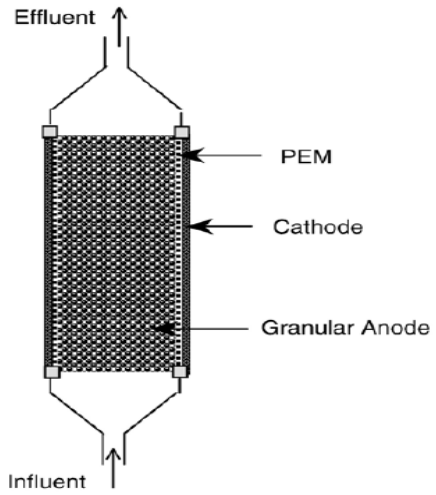

Figure 2-4: Tubular microbial fuel cell with outer cathode and inner anode consisting of graphite granules (Du et al., 2007)

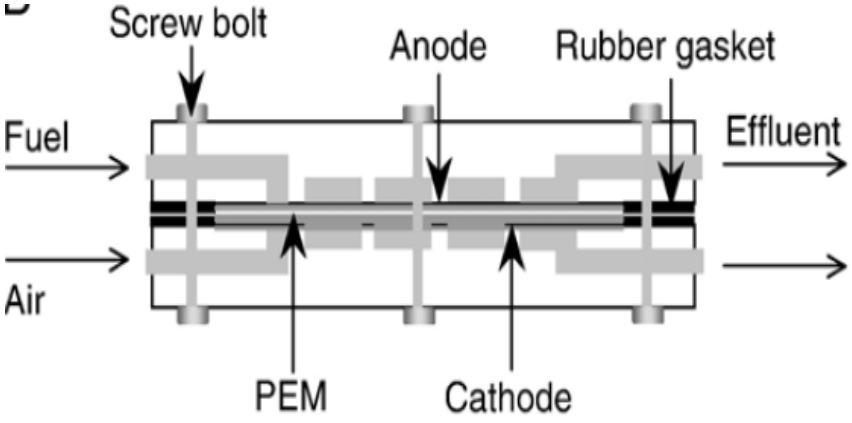

Figure 2-5: Schematic of a flat type microbial fuel cell (Du et al., 2007)

Table 2.1 shows the example of basic components of microbial fuel cells

Table 2-1: Basic components of microbial fuel cells

Items	Materials	Remarks
Anode	Graphite, graphite felt, carbon paper, carbon cloth,	Necessary
Cathode	Graphite, graphite felt, carbon paper, carbon cloth	Necessary
Anodic chamber	Glass, polycarbonate, plexiglass	Necessary
Cathodic chamber	Glass, polycarbonate, plexiglass	Optional
Proton exchange system	Proton exchange membrane: Nafion, ultrex, polyethylene, salt bridge	Necessary
Electrode catalyst	Pt, Pt black, MnO_2	Optional

(Source: Du et al., 2007)

MFCs exhibit key advantages over technologies currently used for producing electricity utilizing organic matter. First and foremost, high conversion efficiency is ensured in the direct conversion of substrate energy to electricity. Besides, gas treatment is not required in MFCs as off-gases of MFCs are enriched in carbon dioxide (CO_2) and have no useful energy content. Moreover, MFCs can operate at ambient and even at low temperature which differentiating them from the current bioenergy processes. In addition, there is no energy requirement for aeration whereby the cathode is passively aerated in MFCs (Liu et al., 2004). This is the notable feature exhibited by MFCs as aeration alone can account for half of the operation costs at a typical treatment plant (Logan, 2008). At last, MFCs is a promising technology for widespread application in places lacking of electrical infrastructures and as the alleviation to the energy crisis currently being encountered by expanding the diversity of energy resources (Rabaey and Verstraete, 2005).

The present status of power generation by MFCs is presented in Figure 2.6. It can be seen that given the low working volume of MFCs, higher power density is generated than the high volume systems. In the range of 10 to 100 mL, the maximum power generation achieved was in the range of 100 to 500 W/m^3. Looking at the types of substrates used as shown in Figure 2.7, the power generated by MFCs dropped from

that using simple substrate such as glucose (100 W/m^3) to 10 W/m^3 of that with complex substrate like industrial wastewater.

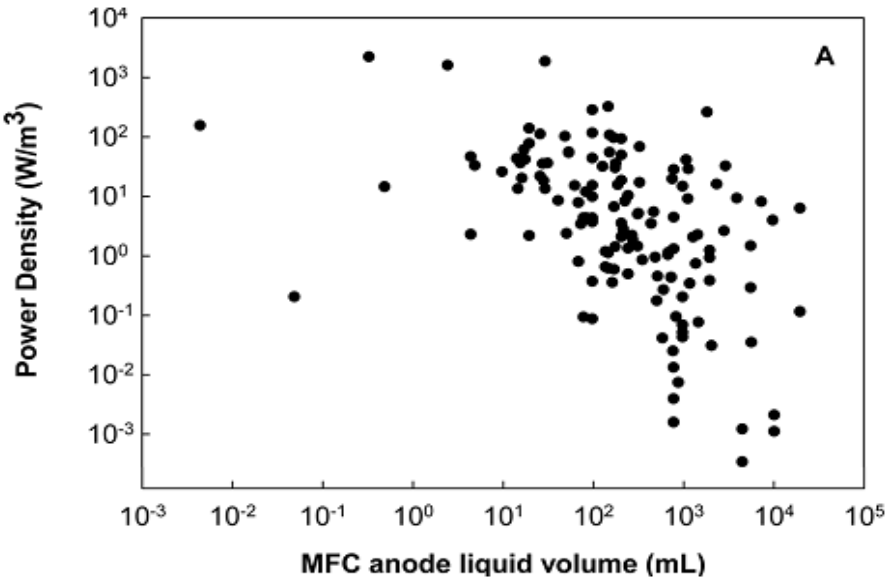

Figure 2-6: Electricity generation in microbial fuel cells with different anode liquid volumes (Ge et al., 2012)

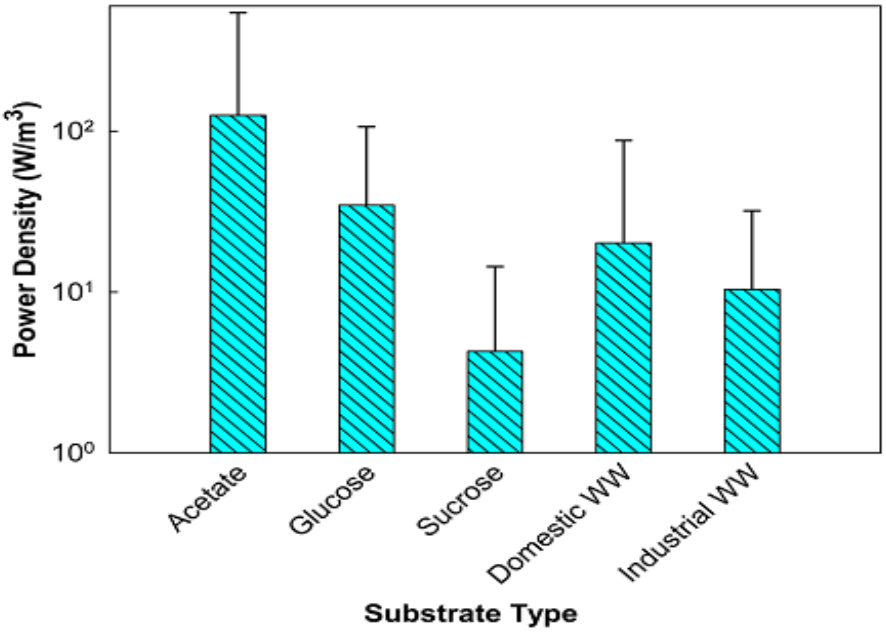

Figure 2-7:Power density by microbial fuel cells treating different types of substrates (Ge et al., 2012)

Garnering knowledge on MFCs is essential for optimizing energy production from MFCs and future development of it.

2.3 Factors Influencing Microbial Fuel Cell Performance

To access the performance of MFCs, it depends on a complex system of parameters including types and concentrations of substrate, types of inoculum, pH of substrate, conductivity, microbial activity, circuit resistance, electrode material, electrocatalyst, and membrane material (Liu et al., 2005).

2.3.1 Microbial Metabolism

According to Schroder (2007), energy efficiency of MFCs is associated with the mechanisms of electron transfer occurred in anode of MFCs. In other words, the exploitation of every living cell to dispose the electrons liberated during substrate disintegration is the basis to the mechanism of microbes' metabolism. Metabolic routes governing proton flows as well as microbial electron. The electrons to be delivered towards the electrode need a physical transport system for extracellular electron transfer. According to Delaney et al. (1984), that can be happened through the use of soluble electron shuttles or through membrane-bound electron shuttling compounds (Vandevivere and Verstraete, 2001). On the other hand, the anode potential will determine the bacterial metabolism, subsequently redox potential of the final bacterial electron shuttle and hence metabolism. A number of different metabolism pathways can be classified based on the anode potential including fermentation, high redox oxidative metabolism, and medium to low redox oxidative metabolism. Microbes used in MFCs reported to date comprises of aerobes, facultative anaerobes and strict anaerobes (Rabaey and Verstraete, 2005). Table 2.2 summarized the kind of microbes used in MFCs.

Table 2-2: Summary of microbes used in microbial fuel cell

Microbes	Substrates	Applications	Reference
Actinobacillus succinogenes	Glucose	Electron mediator	Park and Zeikus, 2000
Aeromonas hydrophila	Acetate	Mediator-less MFC	Pham et al., 2003
Pseudomonas	Glucose	Self-mediate consortia isolated	Rabaey (2004)

aeruginosa		from MFC	
Clostridium beijerinckii	Starch	Fermentative bacterium	Niessen et al. (2004b)
Desulfovibrio desulfuricans	Sucrose	Sulphate/sulphide as mediator	Park et al., 1997)
Geobacter metallireducens	Acetate	Mediator-less MFC	Min et al. (2005a)
Rhodoferax ferrireducens	sucrose, maltose	Mediator-less MFC	Liu et al., 2006)

2.3.2 Types of Substrates

Apart from microbial metabolism, substrate is regarded as one of the prime factors affecting MFC power generation (Liu et al., 2009). Substrate serves as carbon or nutrient and energy source. According to Angenent and Wrennn, efficiency of converting organic wastes to bioenergy depends on the chemical compositions as well as concentrations of the components of waste material (2008). A broad spectrum of substrates can be used in MFCs system for power generation ranging from pure compounds such as glucose and organic acids, acetate, to complex mixtures of organic matter present in industrial, domestic, and animal waste wastewater.

Acetate, being the simple substrate (Bond et al, 2002), has been utilized extensively as the recalcitrance of multitude kinds of wastewater making them more difficult to be used as substrate for electricity generation (Sun et al., 2009b). Besides, acetate is inert towards alternative microbial conversions like fermentations and methanogenesis at room temperature (Aelterman, 2009). Chae et el. demonstrated that MFCs fed with acetate showed the highest CE (72.3%), followed by butyrate, propionate, and glucose with readings of 43.0%, 36.0% and 15.0%, respectively (2009).

Another commonly used substrate in MFCs is glucose. A maximum power density of 216 W/m^3 was obtained from a glucose-fed batch MFC using 100 mM ferric cyanide as cathode oxidant (Rabaey et al., 2003). As reported by Hu (2008), a maximum power of 161 mW/m^2 was generated in a baffle-chamber membraneless MFC inoculated with anaerobic sludge and glucose.

Wastewater from breweries with low strength has been a favorite among researchers as a substrate in MFCs due to its food-derived nature of the organic matter such as carbohydrate and low concentrations of inhibitory substances like ammonium nitrogen (Feng et al., 2008). The concentration of brewery wastewater is typically in the range of 3000-5000 mg of COD/L with approximation of 10 times more concentrated than domestic wastewater (Vijayaraghavan et al., 2006). Feng et al. evaluated air cathode MFC performance using beer brewery wastewater added with 50 mM phosphate buffer and achieved a maximum power density of 528 mW/m^2, which was lower than that of using domestic wastewater at similar strengths (2008). This can be accounted for the difference in conductivities of two wastewaters.

Starch processing wastewater (SPW) represents a vital energy-rich resource as it contains a relatively high amount of carbohydrates (2300-3500 mg/L), sugars (0.65-1.18%), protein (0.12-0.15%) and starch (1500-2600 mg/L) (Jin et al., 1998). SPW was used as substrate to enrich a microbial consortium generating current (0.044 mA/cm^2) was coupled to a sharp fall in COD from over 1700 mg/L to 50 mg/L in 6 weeks (Kim et al., 2004). However, there was low columbic efficiency (CE) which might be attributed to oxygen diffusion to the anode compartment resulting in biomass production and fermentation.

Synthetic wastewater with well-defined composition is also used by researchers in MFCs as it is easy to control the loading strength, pH and conductivity. Azo dyes comprise the largest chemical class of synthetic dyes and are extensively present in effluent from textile and dye-manufacturing industries. Removal of dye is of paramount importance as their intense colour contributed to severe environmental problems which consequently causing detrimental effect to aquatic life due to obstruction of light and oxygen transfer into water sources (Pant et al., 2008). Accelerated decolorization of azo dye (active brilliant red X-3B, ABRX3) in a MFC was reported when glucose and confectionary wastewater were used as co-substrates with affected electricity generation from glucose by higher concentrations of ABRX3 (>300 mg/L) (Sun et al., 2009a). This was due to competition between azo dye and the anode for electrons. In order to made application of dye in MFC system possible, efforts required to find appropriate bacterial community that is capable of utilizing a mixture of dyes and other simple substrates.

Landfill leachates are heavily polluted landfill effluents with a complex composition consisting of pollutants, for instances, dissolved organic matter, inorganic macro-components, heavy metals, and xenobiotic organic compounds (Kjeldsen et al., 2002). Zhang et al. generated electricity continuously for 50 hours using leachate in an upflow air-cathode MFC with maximum volumetric power of 12.8 W/m^3 and a current density of 41 A/m^3 (2008). Besides, in work conducted by Greenman et al., it is proven the possible electricity generation and landfill leachate treatment in MFC columns (2009).

Palm oil mill effluent (POME) is a representative of complex substrate. Typically, POME which has a pH ranging from 4 to 5 due to the presence of organic acids is highly polluting attributed by its high content of biochemical oxygen demand (BOD) (10,250-43,750 mg/L), chemical oxygen demand (COD) (15,000-100,000 mg/L), total solids (TS), total volatile solids (TVS), dissolved constituents like amino acids, carbohydrates ranging from hemicelluloses to simple sugars, lipids, inorganic nutrients such as sodium, potassium, and calcium, nitrogenous compounds, etc. (Santosa et al., 2008; Singh et al., 2010). More than 2.5 tonnes of POME is produced for the production of 1 tonne crude palm oil (Ahmad et al., 2003). If POME discharged without treatment, it can lead to adverse environmental problems (Borja et al., 1996).

In Baranitharan et al. work (2013), POME was treated using dual chamber microbial fuel cell inoculated with POME-originated anaerobic sludge where there is higher potential for bioenergy generation from complex POME. Power production is enhanced due to better utilization of substrates by various types of microbes present in anaerobic sludge. Polyacrylonitrile carbon felt (PACF) was used as electrode. Effects of initial chemical oxygen demand (COD) on MFC power generation, COD removal efficiency and coulombic efficiency (CE) were investigated using various dilutions of raw POME and achieved maximum power density and volumetric power density of about 45 mW/m^2 and 304 mW/m^3, respectively, and low CE and COD removal efficiency of around 0.8 % and 45 %, respectively. On the contrary, POME with a ratio of 1:50 dilution showed higher COD removal efficiency (~70%) and CE (~24%) but low power density (~22 mW/m^2) and volumetric power density (~149 mW/m^3). The results show that initial COD has great influence on CE, COD removal efficiency and power generation.

Apart from abovementioned substrates, other substrates have also been evaluated. Effectiveness of electricity generation is reported by Huang and Logan using wastewater from paper recycling plant added with phosphate buffer in MFC and achieved a maximum power density of 672 mW/m^2 and a much lower power of 144 mW/m^2 from unamended wastewater which was mainly attributed to low solution conductivity (2008). Achievement of maximum power density of 261 mW/m^2 using swine wastewater in MFC as substrate was observed (Min et al., 2005). Besides, Zhao et al. investigated the removal of sulfate and thiosulfate in a single-chamber MFC inoculated with *Desulfovibrio desulfuricans* and a maximum current production of 0.115 mA/cm^2 was observed (2009).

The maximum power density produced can be associated with the complexity of the substrate (single compound versus several compounds). Venkata Mohan et al. (2009) reported that the substrate concentration showed remarkable impact on power generation since they are carbon source (electron donor) for the metabolic activity. Water bodies containing higher organic matter were able to generate higher power output.

The current production in MFC is related directly to the oxidizing ability of the bacteria on a substrate and the transfer of electrons resulting from the oxidation to the anode electrode. The current and power density, columbic efficiency (CE), and pollutants removal efficiencies (COD) differ due to different experimental conditions including initial wastewater composition and concentration, and MFC set up conditions achieved using various substrates in MFCs. Generally, complex substrates are harder for microbial disintegration and this reflected in lower power generation than acquired from simple substrates. Simple substrates show high CE as well as high COD removal efficiency than the complex substrates. The high CE indicates that the majority consumption of the COD was associated with power generation.

Table 2-3: Summary of microbial fuel cell performance with different types of substrates

Substrates	Power density, mW/m^2	Reference
Acetate	506	Liu et al., 2005
Glucose	161	Hu et al., 2008
Swine wastewater	261	Min et al., 2005
Domestic wastewater	146	Liu and Logan, 2004
Paper recycling wastewater	144	Huang and Logan, 2008
Starch processing wastewater	0.044	Kim et al., 2004
Palm oil mill effluent	45	Baranitharan et al., 2013

The exact mechanism for the real wastewater is not being reported in literature. However, using simple substrate, glucose, the mechanism of electron generation at anode can be expressed through the following equation.

$$C_6H_{12}O_6 + 6H_2O \rightarrow 6CO_2 + 24H^+ + 24e^- \quad (E^0 = - 0.014V) \qquad (2\text{-}3)$$

(Rittmann and McCarty, 2001)

For complex substrate, the anode potential can be varied. For example, Velasquez-Orta et al. (2011) reported the anode potential of -0.1 V vs Normal Hydrogen Electrode (NHE) using paper mill wastewater at the anode.

2.3.3 Membrane

Another prime factor which could significantly influence MFC performance is membrane separator, one of the key components of MFCs. The use of proton exchange membrane (PEM) in microbial fuel cell is for the migration of the protons generated to cathode apart from acting as physical barrier to inhibit substrate crossover and oxygen diffusion between two chambers of MFCs (Leong et al., 2013). Conventional PEM applied in MFCs include Nafions (Chaudhuri et al., 2003; Min et al., 2005a; Min et al.,2005b; Park and Zeikus, 2000), Hyflons (Ieropoulos et al., 2010), Zirfons (Pant et al., 2010) and Ultrexs CMI 7000 (He et al., 2006; Lee et al., 2012; Rabaey et al., 2003; Sun et al., 2012). These PEM have long been the preferred membrane separators for MFCs due to the ease of conducting protons generated in anode directly into the cathode. Nafion membrane, being the most common PEM as it is chemically and

thermally stable, and has high proton conductivity (Logan, 2008). High proton conductivity featured in Nafion membrane is attributed by the negatively charged hydrophilic sulfonate group attached to the hydrophobic fluoro carbon backbone which promotes proton transport through it (Mauritz and Moore, 2004).

Anion exchange membranes (AEMs) are another kind of separator used in MFCs. Development of AEMs can be related to the attempts to solve problems found in CEM, particularly, pH splitting. AEMs acting as proton carrier which facilitates proton transfer apart from conducting hydroxide or carbonate anions from the cathode to the anode chamber (Arges et al., 2010). For example, RALEX™ AEM avoids proton accumulation in the anode chamber and reduces pH splitting (Pandit et al., 2012). AFN, AM-1and ACS are three different types of AEMs where amongst them, AFN membrane with lowest resistance yielded the highest current density, followed by AM-1 and ACS membrane (Ji et al., 2011). Ji and colleagues also reported that, on the other hand, AM-1and ACS have lower oxygen transfer coefficients and maximum oxygen flux than AFNs (2011). Remarkable good properties exhibited by AEMs included reduced pH splitting issue in the anode chamber (Kim et al., 2007b; Pandit et al., 2012), reduced membrane fouling and cathode resistance attributed by the precipitation of transported cations (Mo et al., 2009), and lower ion-transport resistance (Sleutels et al., 2009). Nevertheless, a major downside of AEMs is that it favors substrate crossover (Pandit et al., 2012). This can promote biofouling formation on cathode surfaces, which consequently reduces MFC performance (Chung et al., 2011; Ghangrekar et al., 2007; Harnisch et al., 2009; Ji et al., 2011; Kim et al., 2012; Liu and Logan, 2004; Tang et al.,2010).

Bipolar membrane is defined as the combination of a cation and an anion membrane joined in series (Logan, 2008). In the work carried out by ter Heijne and coworkers (2006), bipolar membrane was used as separator in order to maintain the desired low pH in the cathode chamber and near-neutral pH at the anode without causing fouling. This is due to the fact that the $Fe3^{+}$ ions in catholyte requires a low pH of less than 2.5 which will foul the membrane separator if cation exchanger membrane (CEM) is used instead.

On the other hand, ultrafiltration (UF) membrane which has many tiny pores has been utilized in MFCs operation. Kim et al. (2007b) found out that UF membrane is outperformed by CEM and AEM with lower power generation aside from having high

internal resistances when being tested in double chamber MFCs. Interestingly, the performance of UF membrane is slightly lower than that when CEM is used in air cathode MFCs, implying the possible use of UF membrane in MFCs only under the condition of developed lower internal resistances.

Porous membranes, for example, glass wools (Mohan et al., 2008) and microfiltration membranes (Sun et al., 2009a) have been used as low cost separators in MFCs. In a study conducted by Mohan research team, single chamber MFCs using cheap glass wool as separators are more cost effective for electricity generation and wastewater treatment as compared to PEM (2008). Porous membranes with porous structure favor the cross-over of bigger molecules, including oxygen and substrate, which is an undesired phenomenon. Despite having a low membrane internal resistance (Sun et al., 2009b), porous membranes cannot last longer due to quick biofouling forming on its surface, resulting in increased membrane resistance. This decisively determines that porous membrane is not ideal to be used as ion exchange membrane in MFCs.

Polymer membrane such as sulfonated polymer membranes, SPEEK membranes which consist of sulfonate groups (Xing et al., 2004) and BPSH membranes (Choi et al., 2012) have seen growing application in MFCs. Xing et al. claimed that SPEEK membranes which are produced by sulfonating PEEK membranes to increase proton conductivity yielded better MFC performance than that of Nafion 117 membrane (2004). On the other hand, BPSH membrane has higher conductivity of protons and more hydrophilic which greatly reduces the degree of fouling. However, these leads to membrane swelling which in turns affect the MFC performance due to substrate cross-over (Choi et al., 2012). The open structure of polycarbonate membranes also allows oxygen to crossover which degrades anaerobic bacteria catalytic activity at the same time (Biffinger et al., 2007).

In order to eliminate the issues of membrane fouling, internal resistance, and limited proton transfer rate, membraneless MFC system seems to be a promising solution. High oxygen and substrate crossover are the obstacles which hamper the practical application of membraneless MFC despite possessing good properties such as zero internal resistance, low membrane fouling and cost effective (Aldrovandi et al., 2009; Zu et al., 2011).

To date, undoubtedly Nafions 117 membrane is still the most commonly used membrane in MFC despite encountering challenges like substrate loss, cation accumulation, and oxygen diffusion (Chae et al., 2007) besides high cost incurred (Ghasemi et al., 2012). A trade-off between internal resistances, substrate crossover and oxygen diffusion is very hard to achieve. It is suggested that Nafions 117 membrane should be modified to improve its properties, for instances, prevent fouling formation, reduce substrate and oxygen crossover (Leong et al., 2013).

2.3.4 Electrode Materials

Electrode is one of the main components in affecting the performance of MFCs. Electrode materials differ in their chemical and physical properties, for instances, surface area, chemical stability, electric conductivity, biocompatibility, and mechanical strength which subsequently will have varied impacts on electrode resistance, electrode surface reaction rate and different activation polarization losses. Hence, it is of utmost importance to utilize ideal electrode materials to promote the performance of MFCs (Zhou et al., 2011). The electrode materials must also be of low cost as well (Wei et al., 2011). Anode electrode materials like graphite rod, reticulated vitreous carbon (RVC), graphite fiber brush, carbon cloth, carbon paper, and carbon felt have commonly been utilized for MFCs (Zhou et al., 2011).

Among these electrode materials, carbon felt characteristics outperformed over other materials. Carbon felt has high electron conductivity, fabric of fiber, thicker, and possesses large porosity in comparison to carbon cloth or paper, which allows more surface area for bacterial growth (Zhou et al., 2011). In a study carried out by Baranitharan et al (2013), polyacrynitrile carbon felt (PACF) was used as electrode material for anode and cathode and 45 mW/m^2 of power density was generated using POME. On the other hand, a power density of 622 mW/m^2 (Jong et al., 2011) and 26 mW/m^2 (Liu et al., 2004) was achieved from that using graphite felt and graphite electrode, respectively. In comparison with the carbon-based materials described above, reticulated vitreous carbon (RVC) is seldom been used in MFCs studies due to its large resistance (Zhou et al., 2011). A power density of 170 mW/m^2 using RVC as the anode material was harvested in an upflow MFC (He et al., 2009). On the contrary, several studies have been attempted to utilise non-carbonaceous electrode material instead of carbon based which are regarded as the more versatile anodes. This can be exemplified

in sediment MFC where stainless steel was used as the electrode which resulted in only a maximum power density of 4mW/m^2 (Dumas et al., 2009). In other words, good conducting material does not necessary guarantee an enhanced MFC performance. Several approaches or modifications of anodes to increase power capacity have been done. According to Logan (2008), the most successful was reported in MFC using an ammonia-gas-modified carbon cloth electrode due to the treatment of 5% ammonia gas which believed to have increased the positive surface charge of the cloth. Table 2.4 summaries the comparison of the characteristics of traditional anode materials in microbial fuel cells.

Table 2-4: Comparison of the characteristics of traditional anode materials in microbial fuel cells

Anode materials	Advantages	Disadvantages	Literature
Graphite rod	Good electrical conductivity and chemical stability, relatively cheap, easy to get	Difficult to increase the surface area	Liu et al., 2005
Graphite fiber brush	Higher specific surface areas, easy to produce	Clogging	Ahn and Logan, 2010
Carbon cloth	Large relative porosity	Expensive	Ishii et al., 2008
Carbon paper	Easy to connect wiring	Lack of durability, fragile	Kim et al., 2007
Carbon felt	Large aperture	Large resistance	Kim et al., 2002
RVC	Good electrical conductivity and plasticity	Large resistance, fragile	He et al., 2005

Similar to anode materials, for cathode materials, they have a significant impact on the power output of MFCs as well. Cathode materials should possess a high redox potential and the electrode surface is ensured to be at positive potentials (Zhou et al., 2011). According to Zhou and his colleagues (2011), there is always stereotype thinking of having a large cathodic surface area would facilitate electrode reactions on the cathode

surface. However, as reported by Oh and Logan (2006), they argued that cathode surface areas had only a minor impact on internal resistance and the power output of MFCs. Graphite, carbon cloth and carbon paper are the typical cathode materials used in MFCs. Generally, modifications have been taken on these cathode materials by coating with catalysts. Expensive catalyst such as platinum has shown widespread application in MFCs cathode but is limited due to high cost. Alternatives, inexpensive and efficient iron phthalocyanine (FePc) oxygen reduction catalysts were investigated and proved to be advantageous for MFCs application. Apart from that, manganese oxides and rutile were also studied which also showing quite promising results. In a nutshell, different electrodes exhibited different behaviours in determining the performance of MFCs. It is believed that the exploration of electrode materials should be prioritized judging from the current development as electrode materials of a reasonable price and excellent performance will have positive implications on the application of MFCs. Table 2.5 shows the electrode materials used in MFCs.

Table 2-5: Electrode materials used in microbial fuel cells

Anode	Cathode	Substrate	Configuration	P_{max}, mW/m^2	Reference
Carbon paper	Carbon paper (0.35 mg/cm^2, Pt)	Swine wastewater	SCMFC	261	Min et al., 2005
Graphite rod	Carbon cloth (0.5 mg/cm^2, Pt)	Primary clarifier effluent	SCMFC	26	Liu et al., 2004
Plain graphite	Plain graphite	Chemical wastewater	DCMFC	125	Mohan et al., 2008

Carbon fiber	Stainless steel net (0.8 mg/cm^2, Pt)	Brewery wastewater	SCMFC	264	Cheng et al., 2006
Carbon fiber brush	Carbon fiber brush	Coking wastewater	DCMFC	51.2*	Luo et al., 2010

*W/m^3; SCMFC-single chamber MFC; DCMFC-double chamber MFC; Pmax-maximum power density

2.4 Air Cathode Microbial Fuel Cells

Amongst all the microbial fuel cells (MFCs) configurations, air cathode MFCs has also been studied for power generation comprehensively by researchers. Air cathode MFCs are a variation of MFCs where the cathode compartment is exposed to the air. Over past decades, researchers have been demonstrated the potential of using air cathode MFCs in generating comparable power and treating wastewater (Cheng et al., 2006c; Wen et al., 2012, Lu et al., 2011, Zhang et al, 2013). As pointed by Lu et al (2011), electron acceptor is among the critical points in determining MFCs' performance where high redox potential materials are used to maximize power generation. Despite a great number of catholytes such as dichromate, persulfate, nitrate and nitride (Virdis et al., 2010), permanganate (Baranitharan et al., 2013), and ferricyanide (Oh and Logan, 2006) have been proposed and tested in MFCs, oxygen still remains as the most ideal candidate as electron acceptor accounted to their higher redox potential, abundance, and non-toxic nature (Wen et al., 2012). Moreover, these high energy catholyte materials are cost inefficient and have low sustainability where replenishment is necessary after certain period of operation (Lu at el., 2011). The distinctive advantages exhibited by air cathode MFCs over double chamber MFCs are there are no requirements for catholyte and extra space to operate. Air cathode MFCs is the best choice for both chemical fuel cells and for MFCs because the reduction product is the clean and non-polluting water (H_2O), due to the reduction of molecular oxygen in cathode. Figure 2.8 illustrates single chamber air cathode MFC.

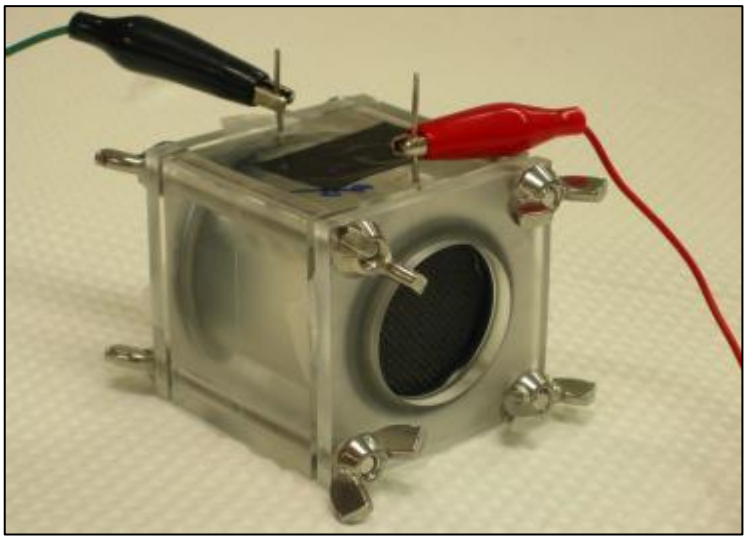

Figure 2-8:Single chamber air cathode microbial fuel cell

Various types of electrochemical reactions can happen at the cathode, for instances, oxygen reduction reaction (ORR) and permanganate reduction reaction (Baranitharan et al., 2013). Despite of the fact that anode is one the limiting factors in MFCs (Logan, 2008), the significance of cathode's role in MFCs' performance cannot be neglected.

In air cathode microbial fuel cell where open air sources is utilized, reduction reaction of oxygen occurs at cathode surface where electrocatalyst plays the most crucial role in obtaining higher kinetic rate and hence better performance. Apart from that, electrochemical principles and laws do govern the power generation of MFCs which always results in lower voltage output and with respect to this, cathodic limitations seem to be intriguing (Yazdi-Rismani, 2008). According to him, several possible causes which attributed to these cathodic limitations have been identified, namely, activation overpotential losses, ohmic losses, and mass transport losses.

2.4.1 Cathodic Limitations of Air Cathode Microbial Fuel Cell

2.4.1.1 Ohmic Losses

According to Logan (2008), ohmic voltage loss is the most important losses to be overcome. It is introduced through the flow of electrons which is hampered by the resistance of the electrode material and membrane (if any) as well as the flow resistance to the ions in the electrolyte to contact points such as wire (Logan, 2008). Ohmic loss is dominant in electrolytes. It can be decreased through the increase in the ionic

conductivity of the electrode and buffering capacity, minimization in contact losses and electrons travel distances between the two electrodes which leads to higher efficiency in electron conduction (Cheng et al., 2006b).

2.4.1.2 Mass Transport Losses

Mass transport or concentration losses which limit the rate of reaction and consequently the current production in MFCs can be accounted for the insufficiency in the species transferred from and to the electrode (Yazdi-Rismani, 2008). This is significant in term of proton flux from the anode. However, the substrate flux to the anode has yet to be reported as an apparent issue as evidence is available for power generation in MFCs. There is always possible that due to proton accumulation caused by proton flux from the anode, the local pH will be lowered and contributed to adverse bacterial kinetics (Kim et al., 2007b). She also stated that power generation might be as well limited due to proton transfer to cathode which is restricted by mass transfer. Mass losses can be minimized through maintaining sufficient buffer capacity aside from minimizing the build up of material on cathode (Logan, 2008). As noted by Oh et al (2004), cathodic overpotential caused by a lack of DO for the cathodic reaction still limits the power density output of some MFCs.

2.4.1.3 Activation Overpotential

According to Logan et al. (2006), an energy barrier is required to be overcome by the reacting species for initiating the oxidation and reduction reactions, including the transfer of electrons produced from anode of MFCs to the electrode or terminal electron acceptor. This energy barrier attributes to activation overpotential or commonly known as voltage loss. It is considered as a limiting step where there is slow reaction kinetics dominating the electrochemical reaction rate at electrode surface. Activation losses are characterized by an initial sharp decline of the cell voltage at the commencement of the electricity generation or in other words, dominant at low current density. Other losses such as ohmic and mass transfer losses get proportionally more important along with the steady increase in current.

By adding mediators, voltage losses due to microbial metabolism can be overcome. In mediator-less MFCs, activation polarization is minimized due to the presence of conducting pili. For example, platinum (Pt) is preferred over a graphite cathode for

performance purpose due to its lower energy barrier in the cathodic oxygen reaction that produces water (Logan, 2008).

2.4.2 Oxygen Reduction Reaction

At the air cathode of microbial fuel cell, reduction occurs. Cathodic reduction can be grouped into aerobic and anaerobic. In aerobic cathodes, oxygen reduction reaction (ORR) takes place when electrons and protons transferred from anode react with oxygen molecule to form water molecules (Min and Logan, 2004). Air cathode microbial fuel cell, as the name implies, oxygen from air is used as terminal electron acceptor due to its abundance, limitless availability, inherent high oxidation potential, sustainability, and passive aeration where no external energy input is demanded (Zhang et al., 2011). The reduction of oxygen is the most dominant electro-chemical reaction at the surface of cathode electrodes.

Two processes can occur during cathodic oxygen reduction. The production of water molecule (H_2O) is the desired four-electron pathway reaction and is expressed through equation as shown below.

$$O_2 + 4H^+ + 4e^- \rightarrow 2H_2O \qquad (E^0 = 1.229\ V) \qquad (2\text{-}4)$$

(Logan et al., 2006)

Whereas, the undesired pathway of a two-electron reaction resulted in the formation of hydrogen peroxide (H_2O_2) is shown in equation below.

$$O_2 + 2H^+ + 2e^- \rightarrow H_2O_2 \qquad (E^0 = 0.695\ V) \qquad (2\text{-}5)$$

(Logan et al., 2006)

Ultimate target for the application of electrocatalyst for ORR is to reach the four-electron pathway reduction reaction at reasonably low overpotential as this has direct impact on current density produced and consequently overall performance (Wang et al., 2005). The ORR of good, new, non-Pt catalysts should follow the 4-electron pathway as closely as possible. According to Yasdi (2008), incomplete reduction of oxygen leads to high overpotential and results in low energy conversion efficiency and generation of

reactive intermediates and free radical species which can be destructive. Normally, the reaction rate of oxygen reduction which involves adsorption and charge transfer is slow due to its sluggish kinetics (Chen et al., 2006; Qiao et al., 2010). Indeed, this is the bottleneck found in power generation in air cathode microbial. Initially, oxygen is adsorped on the surface of the electrode catalyst before the oxygen is further reduced to hydrogen peroxide and water. It is believed that the dissociation of the O-O bond in the peroxyl radical formed initially is the rate-determining step in ORR (Gasteiger et al., 2004).

The power production in MFCs subjects largely on the kinetics of the reduction taking place at the cathode. The reaction kinetics is limited by an activation energy barrier which hampers the conversion of the oxidant into a reduced form. When current is drawn from a fuel cell, activation loss is arose to overcome this activation barrier. Therefore, improved cathodic reaction rates is said to have positive impact on the efficiency and power output of MFCs. The use of catalysts on the cathode surface can lower the cathodic activation overpotential and thus increase the current output of MFCs. It is, therefore, of utmost importance, catalyst is necessitates for the oxygen reduction reaction to speed up the reaction in order to achieve optimum performance in MFCs (Zhang et al., 2013).

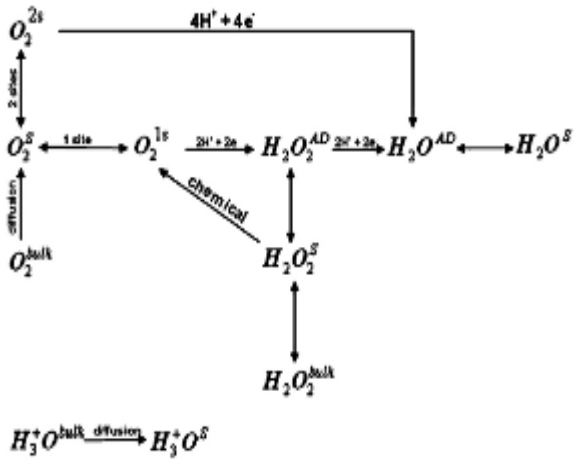

Figure 2-9: Oxygen reduction reaction mechanism (Zhang et al., 2009)

2.4.2.1 Platinum-based Electrocatalyst

The low oxygen reduction reaction (ORR) kinetic in air cathode microbial fuel cells (MFCs) necessitate electrocatalyst to accelerate the reduction reaction which plays a significant role in current generation and hence overall performance of MFCs. To

further improve the performance of MFCs, electrocatalyst which is the heart of air cathode MFC is being studied. Metal catalyst which possesses good electron conductivity and hence electrocatalytic activity, for instance, noble platinum (Pt) has found its widespread use as catalyst for ORR in air cathode MFCs (Steele and Heinzel, 2001; Yazdi et al., 2008; Harnisch et al., 2009). Rigsby et al. (2008) pointed out that platinum exhibits high electrocatalytic activity and stability. According to Yazdi et al. (2008), platinum is the most commonly used catalyst because it has a favorably low overpotential for reduction of oxygen. This is in coherence with study done using Pt as cathodic catalyst where optimum power density is achieved.

In the study conducted by Van et al. (2011), $Ti_{0.7}Mo_{0.3}O_2$ supported platinum catalyst ($Pt/Ti_{0.7}Mo_{0.3}O_2$) was evaluated its catalytic ability. Positive result was obtained as high current density generation was observed. In addition, they did the comparison with Pt/C and PtCo/C catalysts under the same experimental conditions. Better catalytic ability was noticed in $Pt/Ti_{0.7}Mo_{0.3}O_2$ which outperformed the other two catalysts. This findingcan be explained by the fact that $Pt/Ti_{0.7}Mo_{0.3}O_2$ electrocatalyst possesses higher surface area and porosity for oxygen adsorption in ORR. Similarly, Park and Seol (2007) found that Nb-TiO_2 supported Pt catalyst (Pt/Nb-TiO_2) showed well dispersion of Pt nanoparticles with size of 3 nm on the 10 nm Nb-TiO_2 nanostructure supports. The Pt/Nb-TiO_2 showed a comparable catalytic activity for oxygen reduction with carbon supported Pt (Pt/C) catalyst. The enhanced catalytic activity displayed by Pt/Nb-TiO_2 was suggested mainly due to well dispersion of Pt nanoparticles on Nb-TiO_2 nano-size supports. Moreover, the improved catalytic activity may be attributed by an interaction between oxide support and metal catalyst. Apart from that, in the study performed by Wang et al. (2009) using Pt-Fe_3O_4 nanoparticles, there was a 20-fold increase in the oxygen reduction activity compared to that of Pt standalone nanoparticles. In other words, they successfully demonstrated that Pt nanoparticles in Pt-Fe_3O_4 showed higher catalytic activity than the single component Pt nanoparticles for ORR.

On the other hand, according to Mukerjee et al. (1995), PtCr/C, PtFe/C, PtMn/C, PtCo/C, and PtNi/C Pt alloy catalysts demonstrated enhanced performance for ORR. These enhanced electrocatalytic activity of Pt alloy catalysts for ORR is accounted for the high dispersion of the alloy catalysts, disordered structure, and favourable Pt-Pt mean interatomic distance caused by alloying (Hui et al., 2004). Similar result also been reported from a study focused on carbon supported bimetallic catalysts, Pt/Ni with

different Pt and Ni atomic ratios. Enhancement in mass activity for ORR and a lower generation of hydrogen peroxide in pure perchloric acid solution was observed. The advancement in catalytic activity of the Pt-based catalysts might most probably have been originated from the favourable Pt-Pt interatomic distance. Other than binary Pt alloy, Pt-based ternary alloys have also been used as cathodic catalyst. For instances, PtCoCu/C, PtCrNi/C, PtCoNi/C, and PtCoCr/C electrocatalysts have shown positive oxygen electroreduction activity (Seo et al., 2006). Besides, Pt-based quaternary alloy such as PtFeCoCu also being demonstrated to have better catalytic activity over Pt/C (Thompsett et al., 2003). According to Mukerjee et al. (1995), these encouraging performance reported in literatures are mainly due to the increase in Pt d-band vacancy and subsequently decrease in Pt-Pt bond distance which happens through alloying Pt with transition metal whereby eventually leading towards enhancement in oxygen reduction activity.

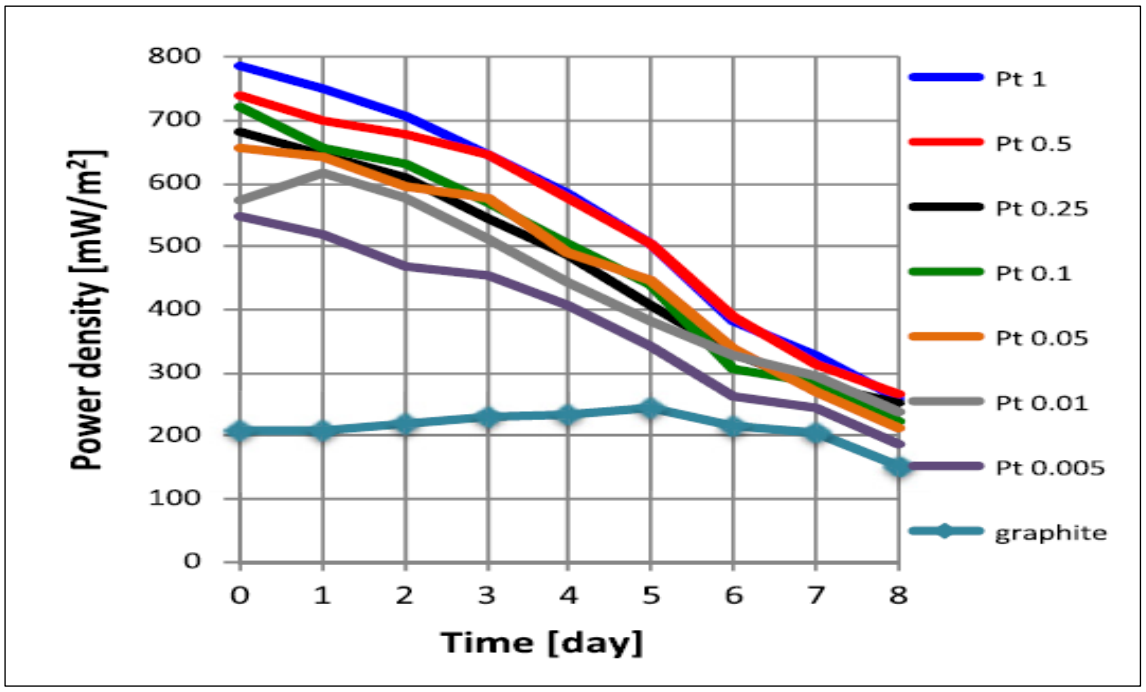

Figure 2-10:Power peaks for the single chamber microbial fuel cells fed with wastewater collected at the University of Connecticut Wastewater Treatment Plant and contained sufficient amounts of electrogenic microorganisms

The most commonly used efficient catalyst is platinum (Pt), but its application is limited due to high cost. Hence, many efforts devoted to reduce cathode cost whereby reducing Pt loading is one of the approaches. From the studies conducted by Santoro et al. (2012), they found that when the Pt loading is decreased from 1 to 0.005 mg/cm^2, an

obvious drop in power generation is observed. However, still, the electricity produced is higher in comparison with graphite. This implies that the aim of sustaining high performance by reducing Pt loading of pure Pt is unachievable.

Similarly, in year 2006, Cheng et al. found that the potential did not change remarkably with a maximum of 19% increase when the Pt loading on the cathode was increased from 0.1 to 2 mg/cm^2 in study using MFC. This can be concluded that Pt modified cathode is remained being competitive and cost-effective.

2.4.2.2 Non-Platinum based Catalyst in Air Cathode Microbial Fuel Cell Platinum-based Electrocatalyst

Widespread application of platinum (Pt) in air cathode MFCs for enhanced performance has been reported. In spite of the high stability criterion displayed through the application of nobel Pt as cathodic catalyst, its practical application is limited due to high cost (Yazdi-Rismani, 2008). As noted, Pt-based catalyst was a major contributor to the cost of MFCs (Zhang et al., 2006). In the efforts of addressing the bottleneck, there has been widespread research and development on non-Pt based electrocatalyst. Pertaining to that, non-precious metals have also been studied as catalysts for improving the kinetics of oxygen reduction reaction in the cathode. The main distinction of using non-noble metals is the cost consideration for future potential scale-up applications of MFCs. These include transition metal macrocyclic compounds, metal nitrides, and metal oxides (Zhang et al., 2013).

In a study focused on the use of ruthenium supported copper (Cu/Ru) catalyst, good oxygen adsorption on its surfaces has been demonstrated from scanning tunneling microscope (STM) image obtained. This indicates that Cu/Ru is capable to be utilized for ORR as cathode catalyst (Wang et al., 2005). Also, in the study using bimetallic catalysts, Pd/Co on glassy carbon for ORR at composition ratio of 90:10, optimum performance was noted. Even though the reaction rate was about half that of Pt/C catalyst, it implies the possibility of Pd/Co as potential electrocatalsyt for ORR (Fernandez et al., 2005). Besides that, in the study using nano-composite, Au-Fe_3O_4, enhanced performance in catalyzing hydrogen peroxide was attained compared to that on either single Au or Fe_3O_4 nanoparticles. This signifies that bimetallic electrocatalyst is a promising catalyst which showed high catalytic activity. However, as this study was focused on hydrogen peroxide reduction, there is no evidence showing the specific

performance of bimetallic catalyst on concerned ORR. As such, study on ORR should be carried out so as to proof its applications on ORR (Lee et al., 2010). It is claimed that cathode reaction has a Monod-type kinetic relationship with the dissolved oxygen concentration (Pham et al., 2004). According to Zhao and coworkers (2005), iron (II) phthalocyanine (FePc) and cobalt tetramethoxyphenylporphyrin (CoTMPP) based oxygen cathodes are cost-effective and are ideal alternatives for use in MFCs as they have been proven similar performances as Pt oxygen electrodes. Improved power output was acquired by increasing catalysts' affinity for oxygen as well as decreasing the activation energy that reduces O_2 to H_2O (Cheng et al., 2006).

Despite of the fact that good performance and positive results were obtained in experiments utilizing non-Pt electrocatalyst, stability and durability of the electrocatalysts are always an issue which subsequently affects the overall performance of the air cathode MFC. The applications of transition metal macrocycles and phthalocyanines have been reported by researchers to have facing hurdles in catalyst stability (ter Heijne et al., 2007). Besides, similar bottleneck also being reported by Bron et al. (2002). They noted that Fe-phenanthroline catalysts employed consumed less than four electrons per oxygen molecule. Instead, hydrogen peroxide was formed through two electrons pathway mechanism and was claimed to have contributed to the low durability of the catalyst. In comparison for the durability issue raised in both Pt-based and non Pt-based catalysts, latter, of higher portion, reduced a higher percentage of oxygen to hydrogen peroxide, which is undesirable in MFCs power generation (Gasteiger et al., 2004). Figure 2.11 and Table 2.6 present the types of non-Pt catalysts used for ORR in air cathode MFCs.

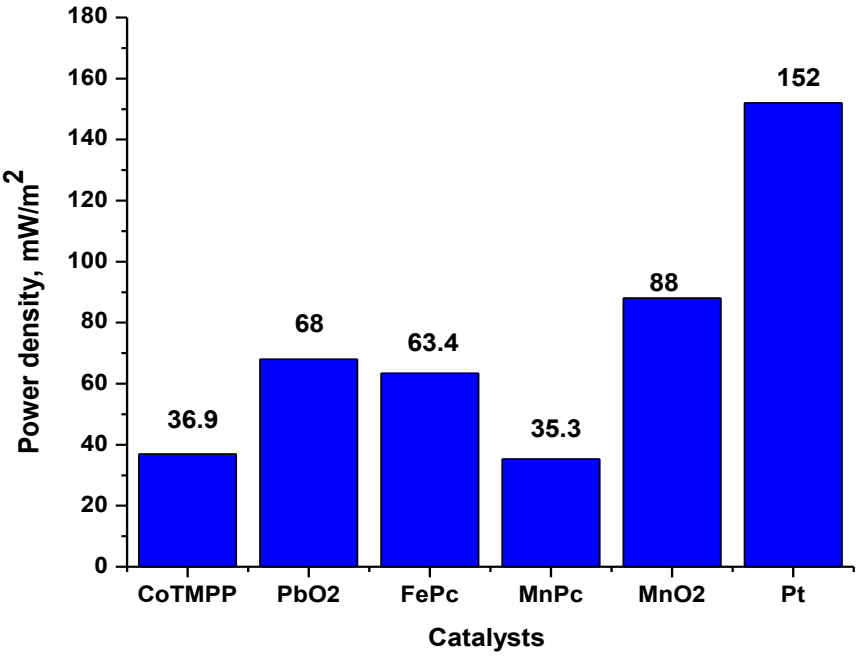

Figure 2-11:Comparison of non-platinum based electrocatalysts with the platinum based catalyst for power generation in microbial fuel cell

Table 2-6: Non-Pt electrocatalysts used in air cathode microbial fuel cell

Catalysts	Cathode materials	Substrate used	OCV, V	P_{max}, mW/m^2	Reference
CoTMPP	Carbon cloth	Glucose	-	36.9	Cheng et al., 2006
PbO_2	Ti sheet	Glucose	-	68	Morris et al., 2007
FePc	Carbon paper	Glucose	0.319	63.4	Yu et al., 2007
MnPc	Carbon paper	Glucose	0.285	35.3	Yu et al., 2007
MnO_2	Carbon cloth	Glucose	0.565	88	Zhang et al., 2009
Pt	Carbon cloth	Synthetic wastewater	-	152	Li et al., 2010

2.4.2.2.1 Performance of Manganese Dioxide in Air-Cathode Microbial Fuel Cell

Among non-platinum based electrocatalysts, according to Espinal et al. (2004), manganese oxides (MnOx) which has found its wide applications in catalysis and molecular adsorption exhibits excellent chemical and physical properties amongst non-noble metal oxides. In addition to that, Kong et al. (2007) pointed out that MnOx, as a

promising catalyst, has high chemical stability and catalytic activity besides being environment friendly and has low cost and toxicity. As mentioned by Zhang et al. (2009), the most effective catalyst was β-MnO_2/graphite among MnO_2 materials studied, attributed by its average oxidation states and highest Brunauer-Emmett-Teller (BET) surface area. In the study of enhanced ORR in a MFC fed with synthetic wastewater as substrate, nano-structured MnOx was used as a cathodic catalyst as a substitution for Pt. The nano-structured MnOx was found to have electrochemical activity in ORR. Even though the power density obtained from the experiment was lower than that of Pt, it can be used for the treatment of waste owe to its capability of producing comparable current density (Liu et al., 2010).

From Figure 2.12 and Table 2.7, few examples of non-Pt catalysts used for ORR have been reported. In comparison with Pt, lower power density was yielded. Manganese dioxide, MnO_2 exhibited the highest power density with a reading of 88 mW/m^3 among non-Pt catalysts, followed by PbO_2 and FePc.

In accordance to the positive performance of MFC utilizing MnO_2 as electrocatalyst, widespread of studies have been reported on the use of MnO_2 as alternative and cheaper catalyst for ORR. And, it was found that there are different methods to synthesis MnO_2 which gave different form of MnO_2, including chemical oxidation, electro deposition, and hydrothermal synthesis. Among these methods, hydrothermal approach is the method which yields most promising result. The results are depicted in Table 2.7 and Figure 2.12 as shown below.

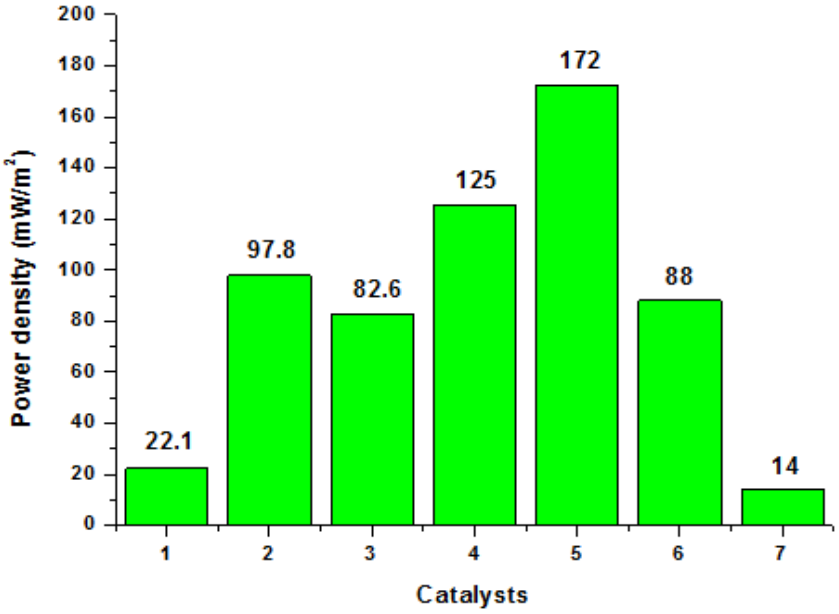

Figure 2-12: Comparison of the performance of MnO_2 electrocatalysts prepared by different methods in air cathode microbial fuel cell

Table 2-7: Use of manganese dioxide as cathode catalyst in air cathode microbial fuel cell

No.	Cathode materials	Catalysts	Preparation methods	Maximum power density, mW/m^2	Reference
1.	Carbon cloth	α-MnO_2	Chemical oxidation	22.1	Lu et al., 2011
2.		β-MnO_2	Hydrothermal synthesis	97.8	
3.		γ-MnO_2	Hydrothermal synthesis	82.6	
4.	Carbon cloth	α-MnO_2	Chemical oxidation	125	Zhang et al., 2009
5.		β-MnO_2	Hydrothermal synthesis	172	
6.		γ-MnO_2	Hydrothermal synthesis	88	
7.	Carbon paper	MnOx	Electro deposition	14	Liu et al., 2010

2.4.2.2.2 Oxygen Reduction Pathway on Manganese Oxides

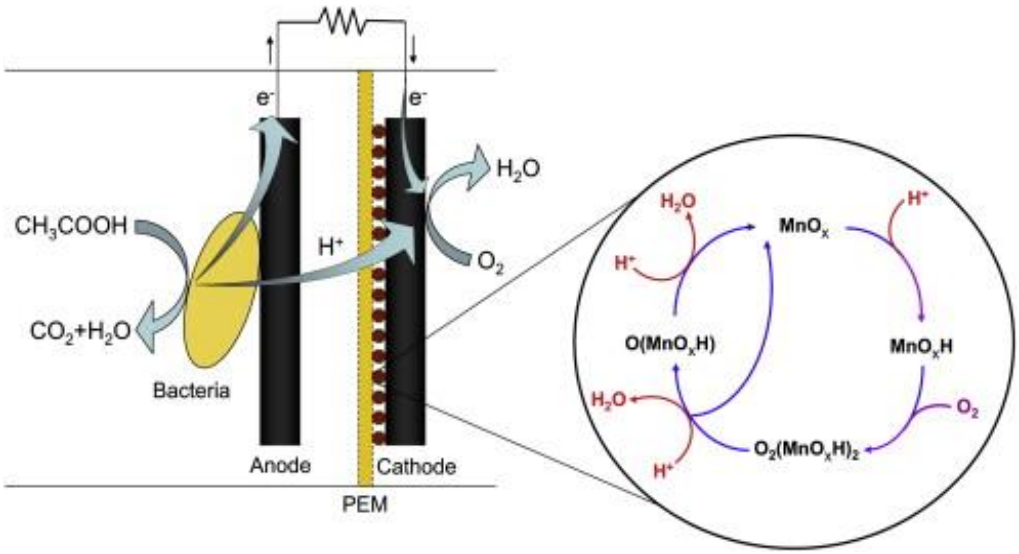

Figure 2-13: Schematic pathways of oxygen reduction on the MnO_x electrocatalyst in a single chamber air cathode microbial fuel cell (Liu et al., 2010)

Understanding of the mechanism on how MnOx works is essential and vital with respect to the use of MnO_2 catalyst for ORR. Figure shows the schematic pathways of oxygen reduction on MnO_x electrocatalyst in a single chamber air cathode MFC. The pathway consists of 4 steps. In the first step, manganese oxide absorbs proton and electron and become manganese oxide complex. After that, as can be seen in step 2 where manganese oxide will be reacting with oxygen molecule to form secondary complex. Proceed to step 3, the secondary complex formed reacting further with electrons and protons, forming adsorption species and at the same time producing water and manganese oxides. And lastly, the adsorbed species formed will be reacting with electron and proton to form water and manganese oxides. Manganese oxides formed in step 4 will proceed further its reaction by repeating again the whole series of reaction starting from step 1. The setback found in MnO_2 is that it is not necessary that the reaction in step 3 will be getting into step 4. In other words, there will be lesser amount of manganese oxides regenerates in case there is no reaction proceeds to step 4. This actually will then contribute to the decreasing power generation nature exhibits by MnO_2 catalyst. The reaction steps are summarized as below.

Reaction 1

$$MnO_x + H^+ + e^- \rightarrow MnO_{x-1}OH$$

Reaction 2

$$2MnO_{x-1}OH + O_2 \rightarrow [(MnO_{x-1}OH)O_{ads}]_2$$

Reaction 3

$$[(MnO_{x-1}OH)O_{ads}]_2 + e^- + H^+ \rightarrow (MnO_{x-a}OH)O_{ads} + H_2O + MnO_x$$

Reaction 4

$$(MnO_{x-1}OH)O_{ads} + e^- + H^+ \rightarrow MnO_x + H_2O$$

(Source: Liu et al., 2010)

2.4.2.2.3 Limitation of Manganese Dioxide in Air Cathode Microbial Fuel Cell

Besides that, MnO_2 also suffering from issues such as low electrical conductivity and low specific capacitance. These two shortcomings possessed by MnO_2 limited the application of it in MFCs with higher loading which consequently will result in low energy density. In addition, instability is also a bottleneck to the use of MnO_2 in MFCs (Hou et al., 2010). With respect to that, efforts have been dedicated for the use of modified MnO_2 in MFCs.

2.4.2.2.4 Modification of Manganese Dioxide

MnO_2 has been modified through several ways such as doping by metal and support with supporting material. Through these modifications, obvious change in performance is observed. As reported by Li et al. (2010), MnO_2 was doped with cobalt, copper and cerium. Among these modifications, a maximum power density of 180 mW/m^2 was generated by MnO_2 doped with cobalt. Whereas for supporting material, MnO_2 supported by carbon nanotubes and graphite nanosheet showed power density of 210 mW/m^2 and 9.6 mW/m^3, respectively, which were higher than that of unmodified ones. Table 2.8 below shows the summary of the performance of MFC utilizing modified MnO_2 catalysts.

`

Table 2-8: Modification on manganese dioxide for oxygen reduction reaction in microbial fuel cell

Modification	Catalysts	Maximum power density, mW/m^2	Reference
Metal doping	Co-OMS-2[a]	180	Li et al., 2010
	Cu-OMS-2	165	
	Ce-OMS-2	35	
	OMS-2	86	
Support material	MnO_2	172	Zhang et al., 2009
	MnO_2/CNTs[b]	210	Zhang et al., 2011
	MnO_2	6.8**	Wen et al., 2012
	MnO_2/GNS[c]	9.6**	Wen et al., 2012

a is manganese oxides with a cryptomelane-type octahedral molecular sieve structure

b is carbon nanotube

c is graphite nanosheet

** values are in W/m^3

2.4 Summary

Wrapping up, it can be said that novel catalyst, platinum (Pt) is the most efficient electrocatalyst for ORR in MFCs to date where its high cost is the hindrance to the widespread application. In the effort devoted for searching of alternative for replacement of Pt, manganese dioxide, MnO_2 was found to be the most prominent one in term of its performance in MFCs. Subsequently, different synthesis pathways have been investigated which resulted in different crystal forms of MnO_2 with different phases and size. Hydrothermal method was found to be able to yield MnO_2 which gives better result. However, due to limitations as well as instability issues reported on MnO_2 for ORR, approaches such as metal doping and supporting with support material were

suggested and have been proven efficient to be used as electrocatalyst for ORR. Hence, in current work, Pt doped on MnO_2 is developed to study for its performance for ORR in air cathode microbial fuel cell

3 MATERIALS AND METHODS

3.1 Chapter Overview

In chapter 3, raw materials and chemicals used in the synthesis of resultant Pt/MnO_2 will be described. Besides, detailed synthesis process of Pt/MnO_2 as well as characterization and analysis associated with Pt/MnO_2 will be explained and discussed with reference to the existing literatures.

3.2 Chemicals and Raw Materials

Potassium permanganate ($KMnO_4$, 99%), sulphuric acid (H_2SO_4, 96%), methanol (CH_3OH, 99%), trisodium citrate dihydrate ($C_6H_9Na_3O_9$, 99%), hexachloroplatinic acid hexahydrate ($H_2Pt_4Cl_6.6H_2O$, 99%), isopropanol (C_3H_8O, 96%), sodium sulphate (Na_2SO_4, 99%), Nafion solution (5 wt%) and digestion solution (0-1500mg/L range; Hach, USA) all of analytical grade were purchased from Fisher Scientific and used without further purification. Polyacrylonitrile carbon felt (PACF) and Nafions 117 membrane were procured from Du Pont (USA). Palm oil mill effluent (POME) and anaerobic sludge were collected from FELDA palm oil plant located at Panching, Pahang. High purity deionized water (18 MΩ cm) was used in all experiments.

3.3 Preparation and Characterization of Catalysts

3.3.1 Manganese Dioxide Preparation

Manganese dioxide (MnO_2) was synthesized by the reduction of potassium permanganate ($KMnO_4$) in aqueous sulphuric acid solution (H_2SO_4) by hydrothermal treatment as described by Yong et al. (2005). Specifically, 4 g of $KMnO_4$ powder was added into 200 mL of 2.5 M H_2SO_4 aqueous solution and was heated at 80°C for 30 minutes under stirring. The precipitates were produced and the solution colour was changed. The reaction course was monitored by the colour change from dark purple to dark brown. The solution was then cooled down to room temperature naturally. Subsequently, the precipitate (MnO_2) was filtered by using filter paper and washed thoroughly with distilled water to remove all the possible remaining ions. Lastly, the precipitate was dried for 48 hours in a vacuum oven (Haier, 2450 MHz, 700 W) at

80°C. Figure 3.1 and 3.2 depict the starting material, $KMnO_4$ powder and the as-prepared MnO_2, respectively.

Figure 3-1:Purplish potassium permanganate powder

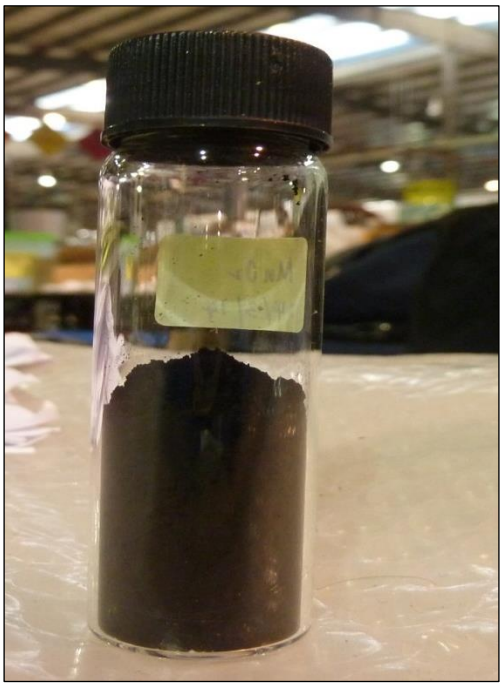

Figure 3-2: As-prepared blackish MnO_2 nanoparticle

3.3.2 Platinum Sols Preparation

Platinum (Pt) sols containing Pt nanoparticles with an average size of 2–3 nm were prepared by the method described elsewhere (Lin et al., 2006). Briefly, a mixture of 5 mL of 0.1 M hexachloroplatinic acid (H_2PtCl_6) aqueous solution and 0.17 g of trisodium citrate dihydrate ($C_6H_9Na_3O_9$) powder was added to 45 mL of methanol solution. The mixture was stirred vigorously under reflux at 80°C for around 30 min. The reaction was stopped by quenching to room temperature immediately after the solution colour turned into dark brown.

3.3.3 Platinum/Manganese Dioxide Preparation and Characterization

Pt/MnO_2 nanostructured catalysts with a Pt loading of 0.2, 0.4 and 0.8 wt%, respectively were prepared by wet impregnation method. In brief, 20 mg of MnO_2 was mixed with 3, 5, and 10 mL of Pt sols each, respectively and ultrasonicated at 65 ^{0}C until the solvents were evaporated, which thereafter, was washed with deionised (DI) water and filtered. The mixture was then dried for 24 hours in vacuum oven (Haier, 2450 MHz, 700 W) at 65 ^{0}C.

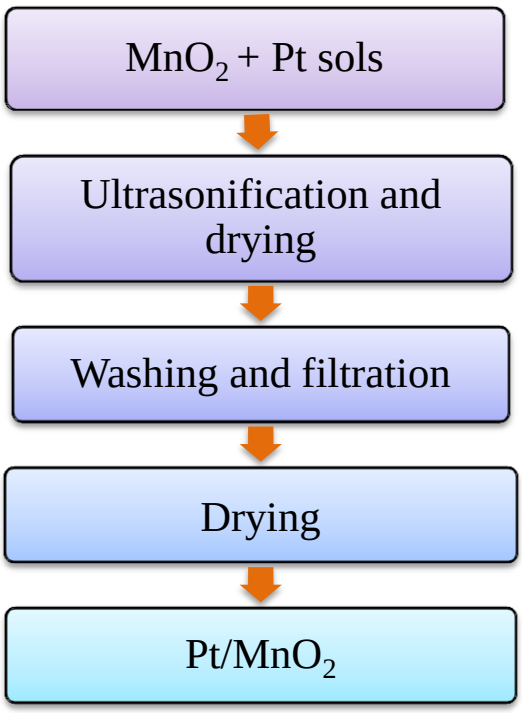

Figure 3-3: Flow chart of the synthesis of Pt/MnO_2

The catalysts synthesized were characterized comprehensively through field emission scanning electron microscope (FESEM), X-ray diffraction (XRD), and X-ray photoelectron spectroscopy (XPS) (XPSPEAK version 4.1) to examine its morphological surface, crystal structure and oxidation states, respectively.

3.4 Electrode Preparation

The electrode was prepared with a catalyst loading of 1.4 mg/cm^2. The prepared catalyst of 10 mg was dispersed evenly on polyacrylonitrile carbon felt (PACF) with a thickness of 2 mm. The area of catalyst dispersion was 7 cm^2. The suspension of catalyst powder for deposition was made by mixing with 0.15 mL of 5 wt% Nafion solution and 0.15 mL of isopropanol (C_3H_8O) and subjected to ultra-sonification for 20 minutes. The Nafions 117 membrane with a dimension of 5 cm x 5 cm was boiled in 0.1 M H_2SO_4 solution for 30 minutes, followed by boiling in deionized water (DI) for 1 hour. The pre-treated membranes were kept in DI water overnight at room temperature before use.

For MEA preparation, catalyst coated PACF and the pretreated nafion 117 membrane were placed between two Teflon papers. The catalyst side was faced to the membrane

side. The hot press was conducted using the hot-press machine (Specac: 6515011) for two minutes at both sides. The press temperature was set at 100 ^{0}C and the press pressure was 1 bar. The steps were repeated in the fabrication of electrodes with different loadings of Pt. A sample without Pt was also prepared and investigated as a control. Figure 3.5 shows the as-prepared MEA on Teflon paper.

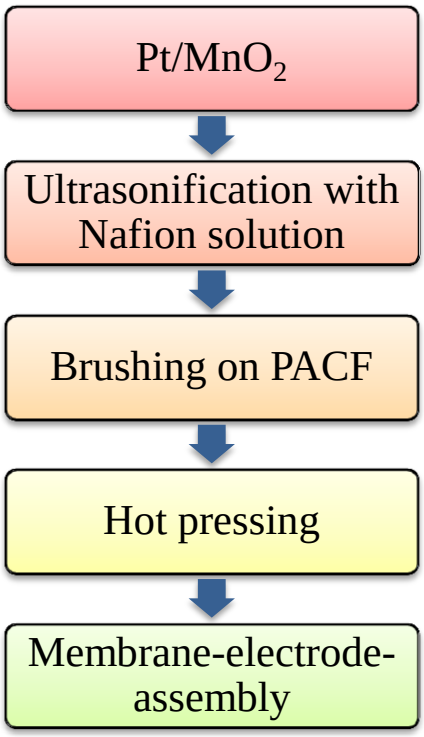

Figure 3-4: Flow chart of preparation of electrode

.

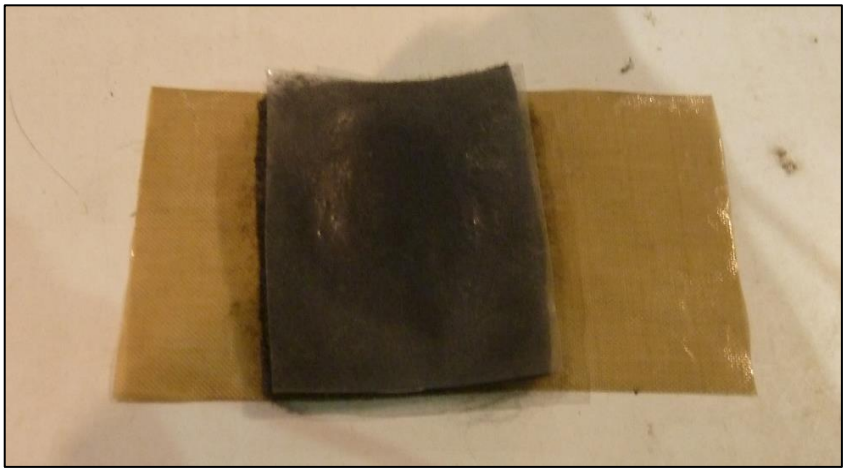

Figure 3-5: Membrane-electrode-assembly (MEA) on Teflon paper

3.5 Microbial Fuel Cell Construction and Operation

The air cathode single chamber microbial fuel cell (MFC) was built with a cubic plexi glass which has a dimension of 5 cm x 5 cm x 5 cm (Shanghai, Sunny Scientific, China) and a total working volume of 20 mL. Carbon brush was used directly as anode electrode. The as-prepared MEA was placed at the front opening side of the cubic chamber by facing the membrane side to the anode substrate and the PACF side was faced to the open air. The whole MFC setup was tighten up with screws. Titanium wire of 5 cm was inserted through the MEA. Electric circuit consisting of resistor was connected from the anode chamber of MFC to the cathode chamber.

The raw palm oil mill effluent (POME) diluted with deionized water (DI) with ratio of 1:49 (Baranitharan et al., 2013) was used as anode substrate of air cathode MFC. Anaerobic sludge was collected from currently running anaerobic digester of oil palm industry (FELDA) located at Panching, Pahang to be used as inoculum in the anode chamber of air cathode MFC. The ratio of anaerobic sludge to the diluted POME is 1:25 (Baranitharan et al., 2013). The anode chamber was flushed with nitrogen gas (N_2) for 1 hour and tightly closed, creating an anaerobic operating condition. For comparing the performance of air cathode MFCs, four air-cathode single chamber MFC reactors with MnO_2, and Pt/MnO_2 of three different loadings were set up for the study. All

experiments were conducted at room temperature. The setup of the single chamber air cathode MFC is illustrated in Figure 3.6 below.

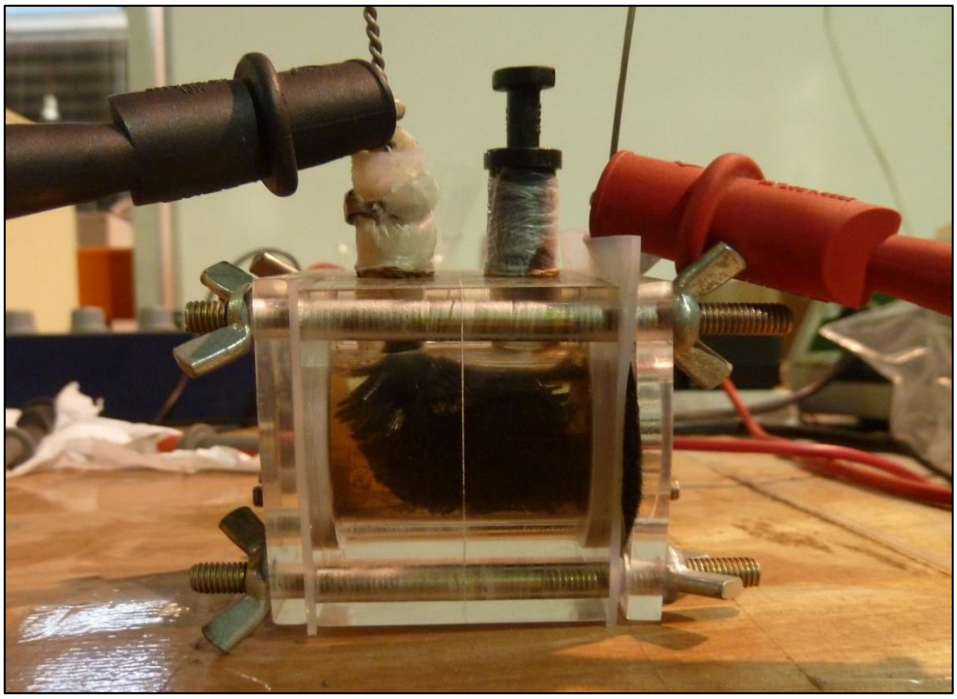

Figure 3-6: Setup of single chamber air cathode microbial fuel cell

3.6 Polarization Measurements and Calculations

Polarization measurements were performed to determine the power generation of MFC at different external resistance ranging from 50 Ω to 500,000 Ω using an external resistor (Fluke 289 true RMS digital multimeters). Polarization curves were obtained from the corresponding voltage data which were taken after the readings stabilized for at least 5 minutes. Power density was normalized to the geometric volume of the MFC (20 cm^3). Power (P, mW), and power densities (P_v,W/m^3) were calculated based on following equations.

$$P = VI \tag{3-1}$$

$$P_v = \frac{V^2}{Rv} \tag{3-2}$$

Where,

V is the cell voltage (V)

R is the external resistance (Ω)

V is the volume of the MFC (m^3)

The open circuit voltages (OCVs) of MFCs were measured after 14 days of MFC operation.

3.7 Chemical Oxygen Demand Measurement of Palm Oil Mill Effluent

For wastewater characterization, required amount of sample was withdrawn from anode chamber after two weeks of MFC operation. The chemical oxygen demand (COD) was determined using digestive solution (0 – 1500 mg/L range; Hach, USA) and measured using a COD reactor (HACH DRB 200, USA) and spectrophotometer (DR 2800, USA).

The COD removal efficiency performance was calculated in term of the percentage of removal. It was done by using the equation as shown below.

$$\text{COD removal efficiency (\%)} = \frac{CODi - CODf}{CODi} \times 100\% \quad (3\text{-}3)$$

Where,

CODi is initial COD reading

CODf is final COD reading at certain day

Figure 3-7: Chemical oxygen demand reactor

Figure 3-8: Spectrophotometer

3.8 Electrochemical Characterization and Analysis

To determine the oxygen reduction reaction (ORR) activity of the catalysts, cyclic voltammetry (CV) was performed using an electrochemical workstation (AUTOLAB 2273, PAR, USA) with a three-electrode configuration consisting of an Ag/AgCl serving as the reference electrode, a working electrode of catalyst coated carbon paper, and a platinum mesh counter electrode placed in 20 mL 0.1 M Na_2SO_4 solution aerated by oxygen for 1.5 hours. Meanwhile, to determine the electrochemical active area, N_2 saturated 0.1 M H_2SO_4 electrolyte solution was used. The scan rate was fixed at 0.03 mV/s. The Pt active surface area was calculated by integrating the charge of the hydrogen desorption region in the cyclic voltammogram, with double-layer charge correction and a conversion factor of 210 Ccm^{-2} Pt.

The working electrode was synthesized by brushing suspension of catalysts on carbon paper with an area of 1 cm^2. The suspension of catalyst made up of 10 mg of catalyst and 0.15 mL of Nafion solution and isopropanol each.

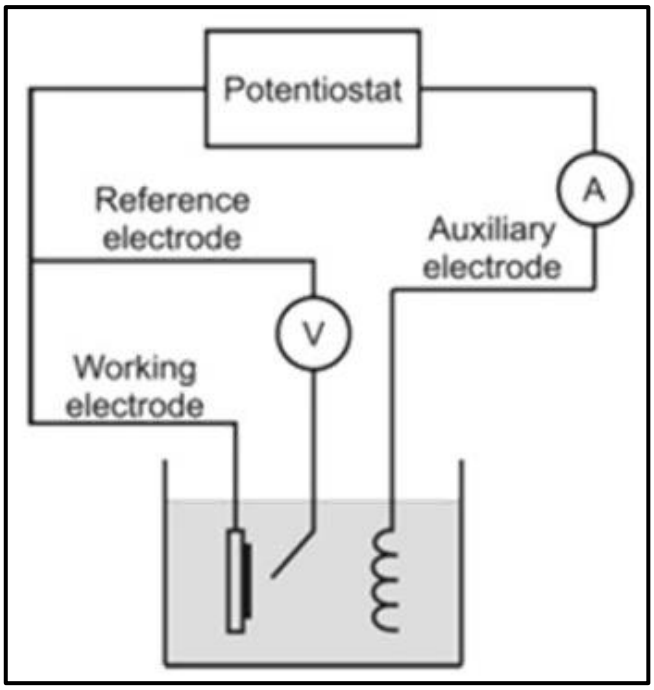

Figure 3-9: Schematic diagram of the CV experiment

3.9 Summary

This chapter describes the chemicals and raw materials used as well as experimental procedures in this study. Details on the materials and chemicals required, step-by-step procedures to synthesize and characterize the catalyst and wastewater, experimental set-up and analysis and calculation to justify the performance of air cathode MFCs were presented.

4 RESULTS AND DISCUSSION

4.1 Chapter Overview

In chapter 4, results of all the characterization and analysis performed will be discussed in detail along with comparison with similar work reported in literature. This includes field emission scanning electron microscope, X-ray diffraction, X-ray photoelectron spectroscopy, cyclic voltammetry, and polarization and power density curves.

4.2 Field Emission Scanning Electron Microscope (FESEM)

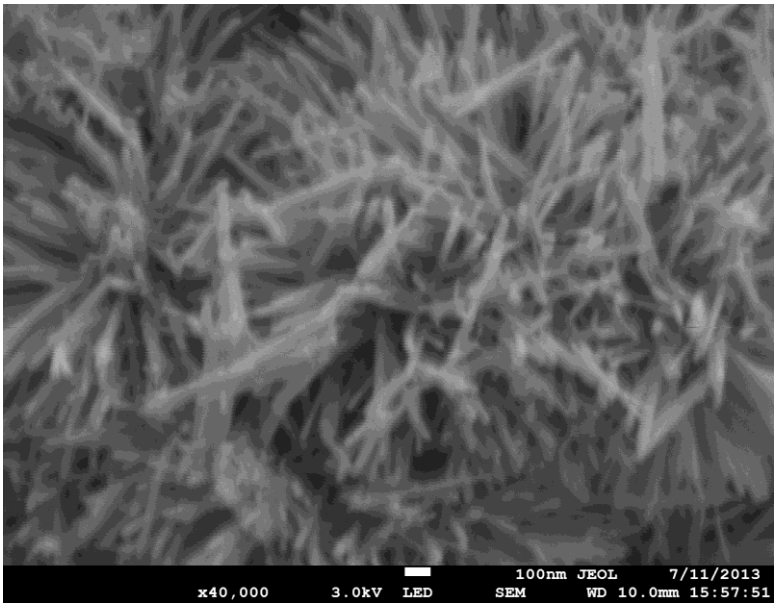

(a)

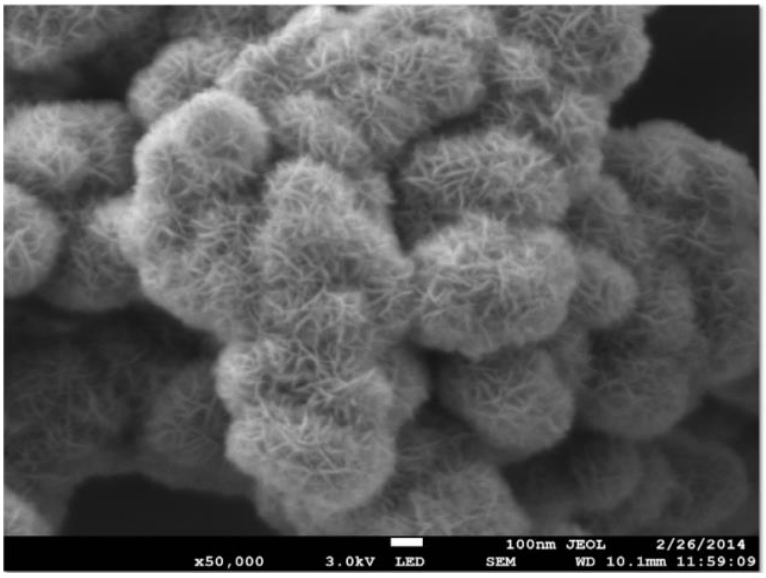

(b)

Figure 4-1: FESEM images of (a) MnO_2 with magnification of 40,000x (urchin-like) (b) Pt/MnO_2 with magnification of 50,000x (cocoon-like)

Field emission scanning electron microscope (FESEM) was performed to determine the surface morphology of the catalysts using .The MnO_2 nanostructure obtained by hydrothermal method resulted in an urchin-like morphology with many long MnO_2 nanorods radiating from its centre (Figure 4.1(a)). After Pt doping from Pt sol, the morphology of the catalyst has been changed as shown in Figure 4.1(b). The Pt/MnO_2 nanostructure showed a cocoon-like morphology. It can be seen that the surface of cocoon-like MnO_2 consists of a large number of short MnO_2 nanorods that interweave with each other. This change in morphology might be due to the sol-MnO_2 powder interaction and further processing such as washing and drying of the nanostructure. The change in morphology from urchin-like to cocoon-like might be advantageous, because the cocoon-like nanostructure possesses higher Brunauer-Emmett-Teller (BET) surface area than the urchin-like nanostructure as reported by Yu et al. (2012).

4.3 X-ray Diffraction Analysis of MnO_2 and Pt/MnO_2 Nanostructures (XRD)

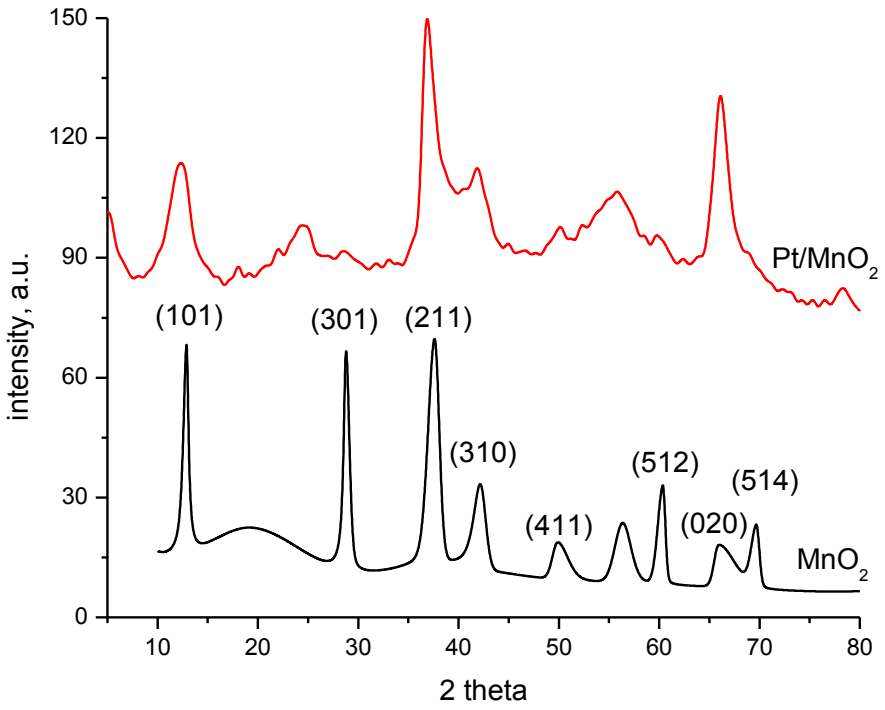

Figure 4-2: XRD patterns of MnO_2 and Pt/MnO_2 nanostructures

The phase, purity and crystallinity of the as-prepared MnO_2 and Pt-MnO_2 were examined by powder X-ray diffraction (D/Max-2500/PC, Rigaku, Japan). All patterns were obtained in the range of two theta (2θ) from 10^0 to 80^0 at a scan rate of 50/min using Cu Kα 1 radiation (λ= 0.154056 nm) with a voltage and current of 40 kV and 40 mA, respectively. The result was illuminated in Figure 4.2, showing nine main peaks of (101), (301), (211), (310), (411), (512), (020), and (514). The sharp diffraction peaks indicate that their crystallinity is high, and the doping process has changed the crystal form. The crystal form of urchin-like MnO_2 can be readily indexed to the pure tetragonal phase of α-MnO_2 (ICDD: 440141), indicating high purity and crystallinity of the final sample with the lattice constants of a=b=9.8093Å and c=2.8324Å from the literature (Yong et al., 2005). Based on the XRD results obtained, the ratio of element O:Mn is 2:1 which is in well agreement with the empirical formula of manganese dioxide (MnO_2). As compared with the XRD patterns of urchin-like MnO_2, the diffraction peaks of Pt/ MnO_2 shifted to smaller diffraction angles. These might be due to the doping process of Pt onto MnO_2 nanostructure.

4.4 X-Ray Photoelectron Spectroscopy (XPS)

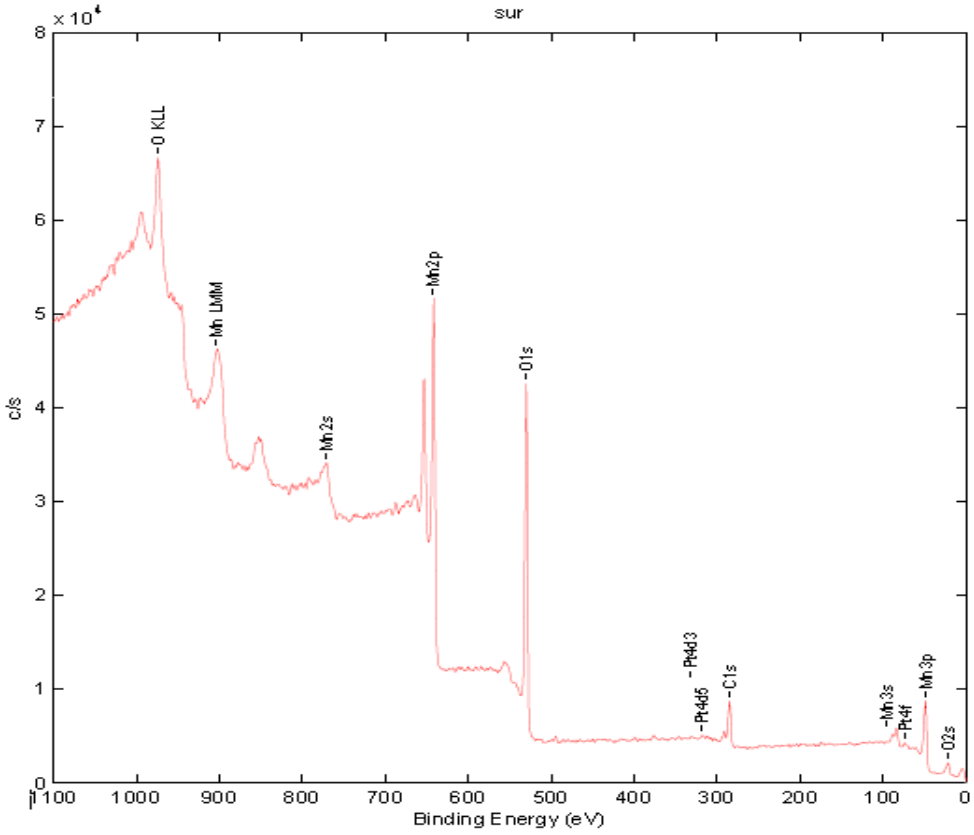

Figure 4-3: Raw data of XPS of Pt/MnO_2 before being deconvoluted

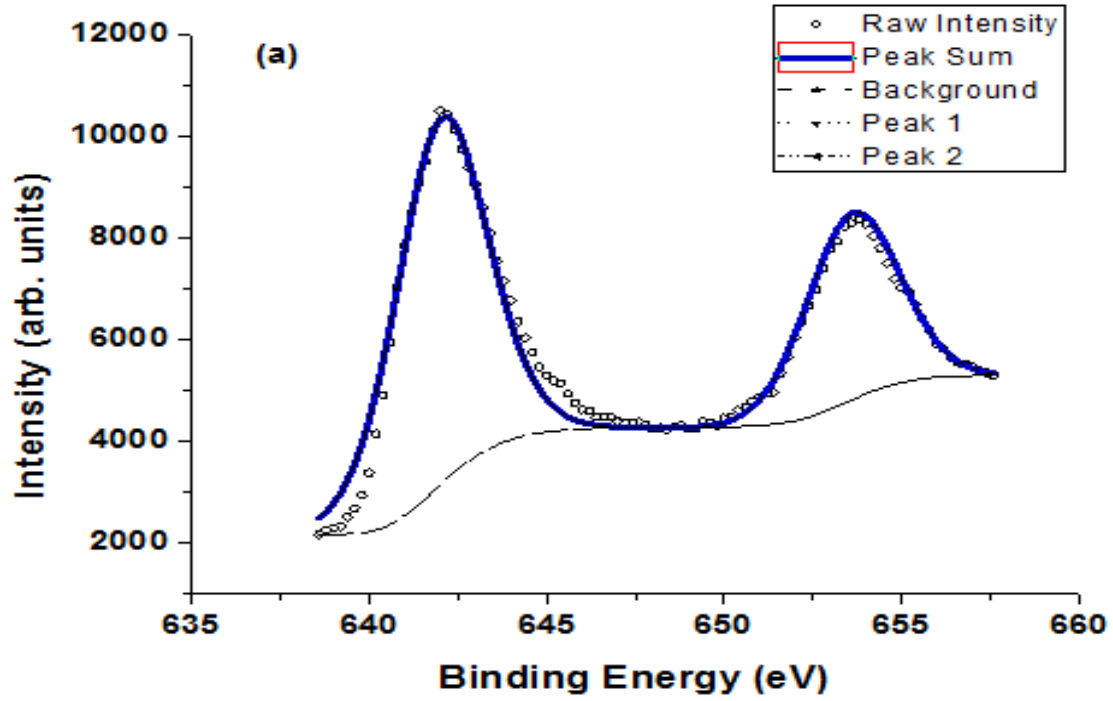
(a)
Raw Intensity
Peak Sum
Background
Peak 1
Peak 2
Intensity (arb. units)
12000
10000
8000
6000
4000
2000
635
640
645
650
655
660
Binding Energy (eV)

(a)

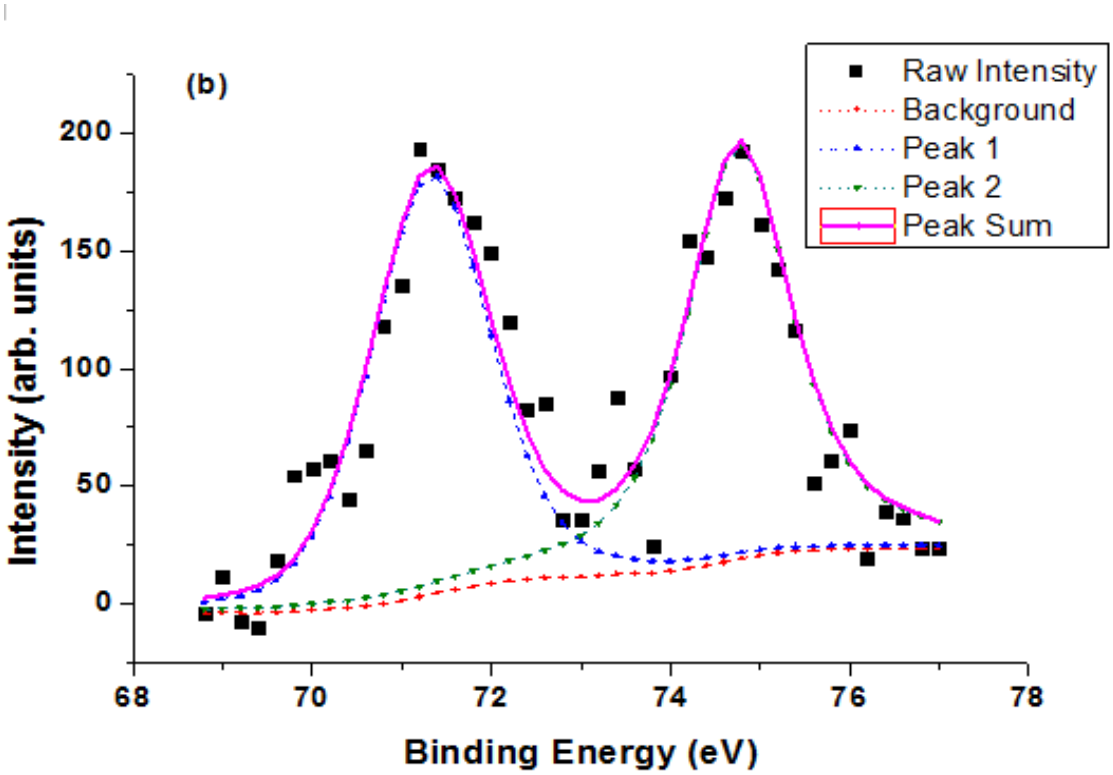
(b)
Raw Intensity
Background
Peak 1
Peak 2
Peak Sum
Intensity (arb. units)
200
150
100
50
0
68
70
72
74
76
78
Binding Energy (eV)

(b)

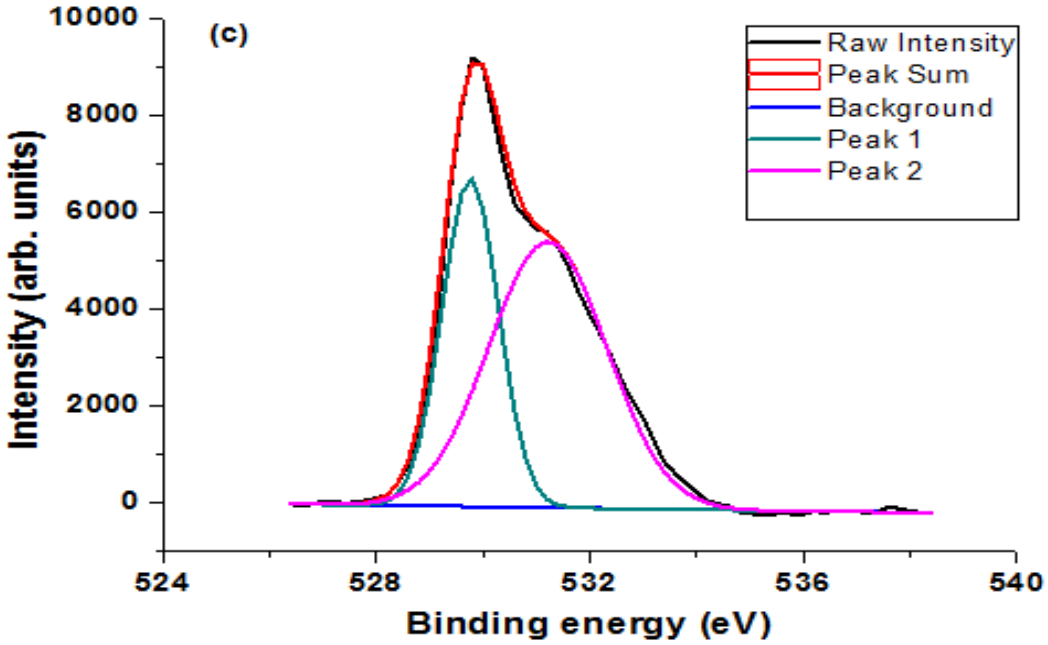

(c)

Figure 4-4: Deconvoluted XPS spectra of (a) Mn 2p (b) Pt 4f, and (c) O 1s region

X-ray photoelectron spectroscopy (XPS) is reported as an effective approach in the investigation of the surface composition and chemical states of solid samples (Li et al., 2003). Besides, information about oxidation state of metal can be obtained through XPS analysis (Ong et al., 2014). A spectrometer was used for X-ray photoelectron spectroscopy (XPS) measurements using KR lines of magnesium (1253.6 eV, 10 mA) as an X-ray source. The peak fittings were done using a Gaussian function with a linear background by using a software XPSPEAK version 4.1 (Wakisaki et al., 2008).

A typical XPS spectrum of Pt/MnO_2 nanostructured catalyst was measured and the core level spectra of Mn 2p, Pt 4f, and O 1s are depicted in Figure 4.4 (a), (b), and (c), respectively. Spectra correction was conducted by using internal reference spectra of adventitious carbon C 1s at 284.6 eV to compensate the electrostatic charging (Awaludin et al., 2011; Barr, 1994; Pawlak et al., 1999). The XPS spectra of Mn 2p for Pt/MnO_2 as presented in Figure 4.4 (a) shows two main peaks centered at binding energy of 642.5 and 654 eV with a difference in binding energy of 11.5 eV. These peaks

could be assigned to Mn 2p3/2 and Mn 2p1/2, respectively (Zhou et al., 2009; Xie and Gao, 2007). The two peaks were in well agreement with those reported in literature, indicating Mn (IV) oxidation state of MnO_2 (Xia et al, 2010; Reddy et al, 2009; Wu and Chiang, 2005). As the starting material used in the synthesis of MnO_2 is potassium permanganate ($KMnO_4$) which has an oxidation state of Mn (VII), and manganese can exist in different oxidation states, hence it is vital to ensure that $KMnO_4$ utilised has been reduced into MnO_2, of which has been proven through XPS for Mn in Pt/MnO_2 nanostructure.

The deconvoluted XPS spectra of Pt 4f for Pt/MnO_2 were illustrated in Figure 4.4 (b). The Pt 4f signal shows two doublet splits due to spin-orbital splitting of the Pt 4f7/2 and Pt 4f5/2 states which were fitted with asymmetric peaks convoluted with Gaussian distribution (Chetty et al., 2009). Two relative intense doublet peaks of Pt 4f7/2 and Pt 4f5/2 were assigned at binding energy of 71.2 and 74.9 eV, respectively. The findings were consistent with the work done by Bera et al. (2003). The pair of peaks is attributed to Pt (0) or Pt metal nanoparticles (NPs) which were also reported in literature (Siburian and Nakamura, 2012; Hull et al., 2006; Delrue et al., 1981; Fleisch et al., 1986). The core level spectra of Pt 4f7/2 and Pt 4f5/2 for the bulk Pt are 70.8 and 74.1 eV, respectively (Awaludin et al., 2011). The fitted spectra of Pt 4f7/2 and Pt 4f5/2 of current work were shifted to higher binding energies with respect to those for the bulk Pt. This discrepancy indicates an electronic interaction of Pt and the substrates, which is MnO_2 in this work (Antolini, 2003). Modification on electronic properties of the surface Pt atom is believed to have occurred. According to Marcini et al. (2007), the positive shift in binding energy is corresponds to a decrease in the electronic charge density on the Pt atoms present in the as-prepared catalysts. This might be attributed to metal-support interactions, where there might be an electron shift from the Pt metal to MnO_2 via π-d hybridization. In addition, as proposed by Toda et al., the enhancement of oxygen reduction currents can be explained by a shift in the d-band electronic density, tuning of the Pt-Pt interatomic distance, and Pt coordination number (1999).

Figure 4.4 (c) displays the deconvoluted XPS O 1s spectra of Pt/MnO_2 centered at 530 eV. The fitting of the spectra gives a sharp peak located at 530 eV and a broad peak at 531.5 eV. The peak at 529-530 eV can be assigned to lattice oxygen while that at 531-532 eV responds to surface oxygen ions or the defect oxygen (Liang et al., 2008).

Similar findings were also reported by Chen et al. (2012). The XPS data analyses of Mn 2p, Pt 4f, and O 1s are summarized in Table 4.1.

Table 4-1: Summary of XPS peak analysis of nanostructured Pt/MnO_2

Species	Peak, eV	Oxidation state	Reference
Mn 2p3/2	642.5	Mn (IV)	Xia et al., 2010
Mn 2p1/2	654	Mn (IV)	Xia et al., 2010
Pt 4f7/2	71.2	Pt metal	Hu et al., 2006
Pt 4f5/2	74.9	Pt metal	Hu et al., 2006
O 1s	530	Lattice oxygen	Liang et al., 2008
O 1s	531.5	Surface oxygen ion	Liang et al., 2008

4.5 Electrochemical Characterization by Cyclic Voltammetry (CV)

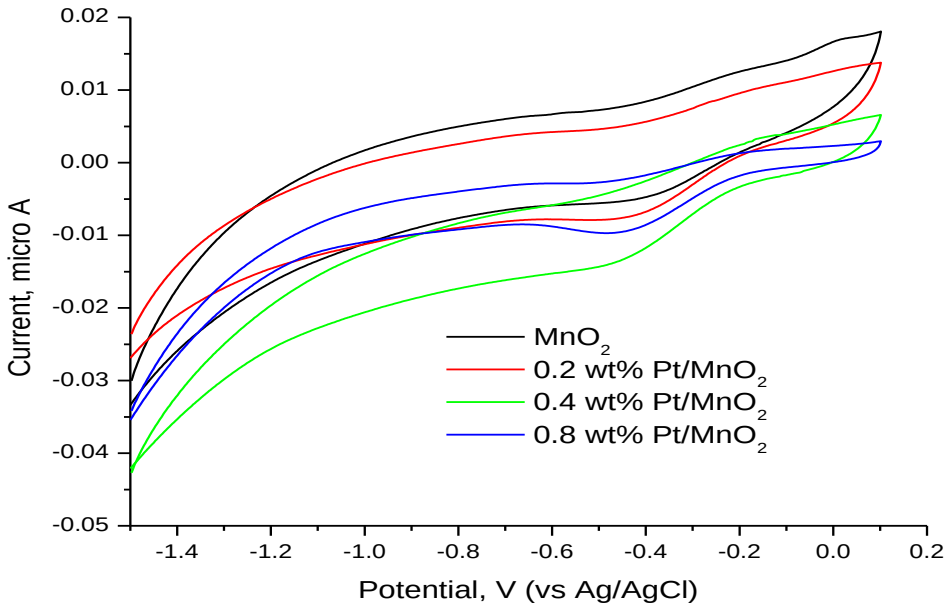

(a)

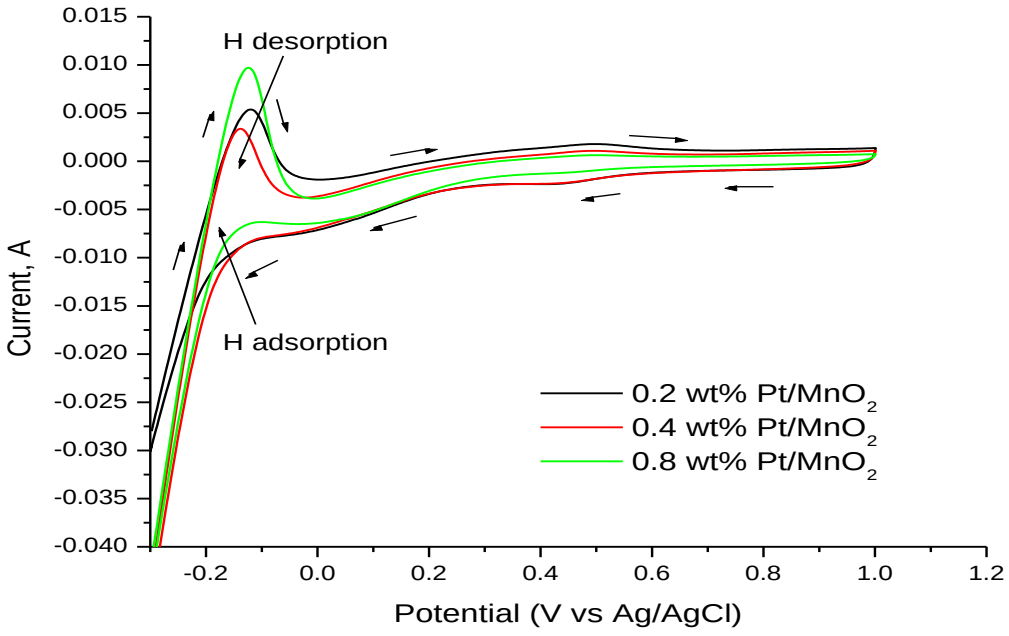

(b)

Figure 4-5: Cyclic voltammograms for (a) ORR in 0.1 mol/L Na_2SO_4 solution saturated by O_2 and (b) electrochemical active area in 0.1 mol/L H_2SO_4 solution saturated by N_2 (scan rate = 30 mV/s)

The electrochemical activity of Pt/MnO_2 was characterized by cyclic voltammogram (CV) approach. The results of the CV of Pt/MnO_2 with different loadings of Pt in 0.1 mol/L Na_2SO_4 solution saturated by oxygen (O_2) are shown in Figure 4.5 (a). An obvious oxygen reduction (ORR) peak of the electrode with MnO_2 and Pt/MnO_2 catalysts is clearly observed at the region of 0.43 to 0.44 V. The peak is slightly positive for Pt doped catalysts than the MnO_2 catalyst, indicating that Pt/MnO_2 catalysts could catalyze ORR at a more positive potential. The ORR current of catalysts are summarized in Table 4.2. The current of the ORR at the electrode with 0.4 wt% Pt/MnO_2 catalyst is -0.013 µA, which is two times higher than that of at the electrode with MnO_2 catalyst with a reading of -0.0056 µA. The higher ORR current of the Pt/MnO_2 catalysts could be explained by the specific interaction between Pt and MnO_2, which is in coherence with the XPS results of Pt 4f species discussed (Fig 4.4(b)).

Meanwhile, the CV results with different loadings of Pt in 0.1 mol/L H_2SO_4 solution saturated by nitrogen (N_2) are shown in Figure 4.5 (b). It was carried out to determine the electrochemical active area of the Pt loading catalysts. From the graph, it can be seen that the H^+ desorption peak in the range of -0.2 to 0 V is evident for all Pt doped MnO_2 catalysts and the area of the peak was increased with the Pt loading. Table 4.2 shows the electrochemical active area of Pt/MnO_2 catalysts evaluated in CV where it can be seen that catalyst with higher Pt loading has higher surface area. The electrochemical active area observed a trend of 2 times increase for 0.4 wt% Pt/MnO_2 catalysts (550 m^2/g), as compared to MnO_2 (276 m^2/g). However, the increment of electrochemical active area was not that much in 0.8 wt% Pt/MnO_2, where there is a sheer 10 % increase be seen (617 m^2/g) as compared to 0.4 wt% Pt/MnO_2. The slight increase in electrochemical active area might be attributed to the increase in platinum nanoparticles size with the increase in the platinum sol volume having the same concentration used. The high active area of the Pt suggests the formation of Pt nanoparticles on MnO_2 catalyst.

Table 4-2: Electrochemical properties of the catalysts

Catalysts	ORR current, μA	Electrochemical active area, m^2/g
MnO_2	-0.0056	-
0.2 wt% Pt/MnO_2	-0.0077	276
0.4 wt% Pt/MnO_2	-0.0134	550
0.8 wt% Pt/MnO_2	-0.0097	617

4.6 Performance of Cubic Air Cathode Microbial Fuel Cell with Different Cathode Catalysts

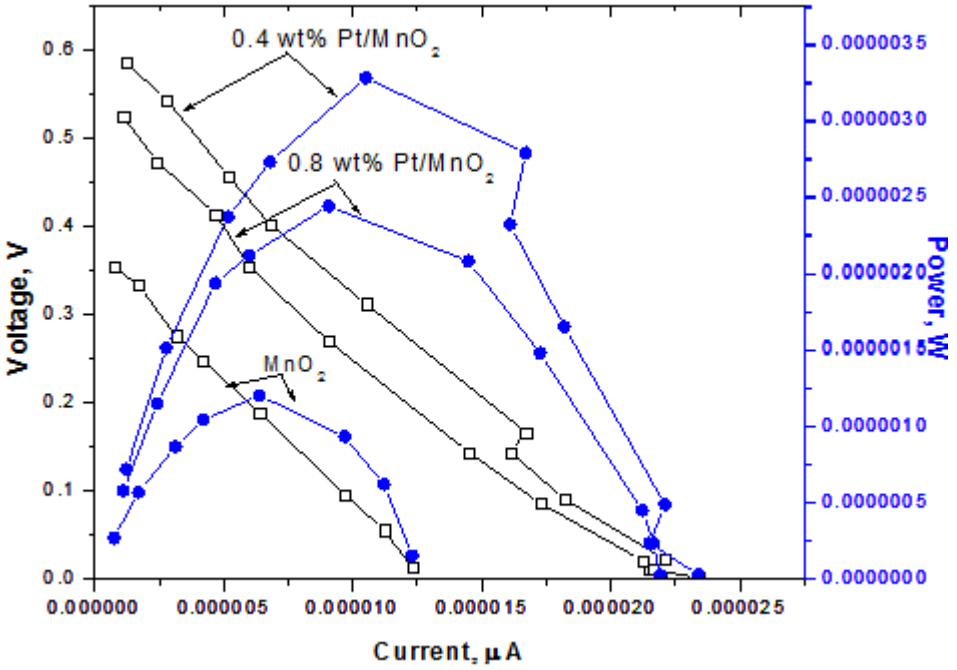

Figure 4-6: Polarization and power curves for air cathode microbial fuel cells after 7 days of operation

Performance of air cathode MFCs with different catalysts were evaluated through polarization curve plotted. Polarization curve is generated to determine the maximum power generation. Similar trend were observed for the cell voltage and current of the MFCs produced. When more resistance was introduced into the MFC system, the current produced will be low meanwhile the cell voltage produced will be high. This can be explained by the fact that the cell voltage was directly proportional to the current density.

The MFCs with different cathode catalysts have been operated continuously maintaining same anode condition and cathode catalyst loading. The open circuit voltage (OCV) and polarization curves were measured regularly. The results are presented in Figure 4.6 and Table 4.3. The power obtained for Pt loadings and MnO_2 catalysts were normalised to the total working volume of MFC cell, giving results in term of power density. It is clearly evident that the maximum power density and OCV are influenced by the cathode, indicating the limiting role of air cathode in the MFC

under the experimental conditions. The performance order of MFCs with different cathodes is 0.4wt% Pt/MnO_2 > 0.8wt% Pt/MnO_2 > MnO_2 cathode as illustrated in Figure 4.16. In other words, maximum power generation occurred in 0.4 wt% Pt/MnO_2 with a reading of 3.25 µW, followed by 2.4µW, and 1.3µW, of that from 0.8wt% Pt/MnO_2 and MnO_2, respectively. The results are consistent with the CV results for ORR activity where highest ORR activity is been observed in 0.4 wt% Pt/MnO_2. The OCVs of the MFC with 0.4 and 0.8 wt% Pt/MnO_2 cathodes were in the range of 0.6 to 0.65 V, which was significantly higher than that of MnO_2 cathode. The electrochemical reaction rates could be evaluated by the open circuit voltage (OCV), as Logan et al. (2006) indicated, a higher OCV value is related to a higher reaction rate, which means 0.4 wt% Pt/MnO_2 exhibits higher rate of reaction. Maximum power density of 0.2 wt% Pt/MnO_2 was not recorded due to the failure of the MFC during the course of operation.

Table 4-3: Performance of air cathode microbial fuel cell based on catalysts

Catalysts	OCV, V	Maximum power density, mW/m^3
MnO_2	0.402	95
0.2 wt% Pt/MnO_2	0.385	-
0.4 wt% Pt/MnO_2	0.626	165
0.8 wt% Pt/MnO_2	0.602	125

Table 4-4: Comparison of microbial fuel cell performances with literatures

Catalysts	OCV, V	Anode substrate	Maximum power density, mW/m^3	COD removal efficiency, %	Reference
α-MnO_2	-	Glucose	367.00	-	Zhang et al., 2009
MnO_2/CNTs	-	Municipal wastewater	112.24	-	Zhang et al., 2009
Pt	-	Barley processing water	174.00	-	Guerrero et al., 2010
α-MnO_2	0.402	Palm oil mill effluent	95.00	78	This work
0.4 wt% Pt/MnO_2	0.626	Palm oil mill effluent	165.00	84	This work

Comparison of the performances of Pt loading catalysts and MnO_2 was conducted with literature and summarized in Table 4.4. In year 2009, in the study done by Zhang et al using simple substrate, glucose and α-MnO_2 as catalyst, a maximum power density of 367 mW/m^3 was harvested. In comparison, by using complex substrate like municipal wastewater and still, MnO_2 based catalyst, a three times decrease in power generation was observed. This can be explained by the truth that lower power generation is expected in MFC utilizing complex substrate. In present study, MnO_2 yielded 95 mW/m^3 by using palm oil mill effluent (POME), which is one of the complex substrates. The result is comparable to that using municipal wastewater. On the other hand, as reported by Guerrero et al (2010), in MFC using novel Pt and barley processing water as substrate, they generated 174 mW/m^3 of power. His work is significant as it implies the maximum power density generated in present work which is close to that with a reading of 165 mW/m^3 is a promising electrocatalyst to be used in air cathode MFCs for treatment of complex substrate, POME.

4.7 Stability of Pt/MnO_2

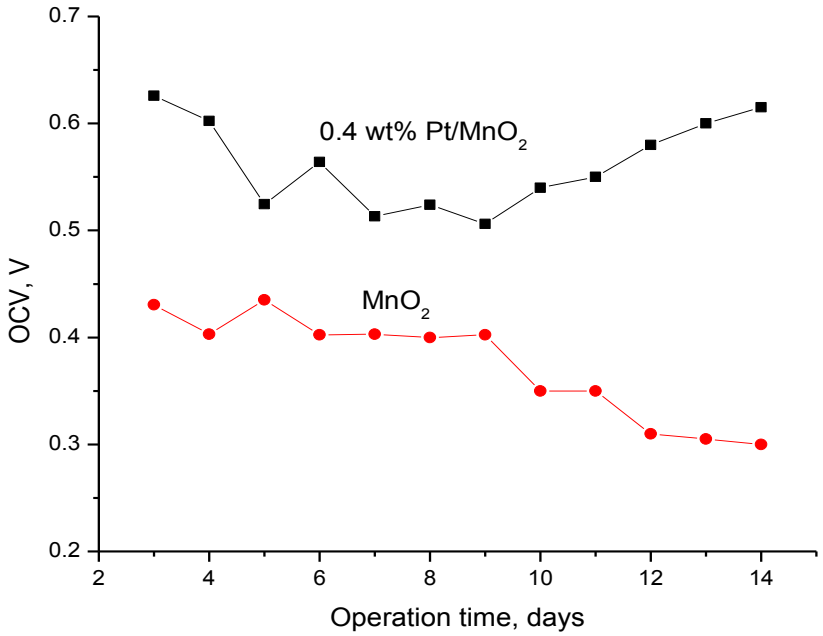

Figure 4-7: Open circuit voltage of microbial fuel cell with Pt/MnO_2 and MnO_2

Figure 4.7 presents the OCV value as a function of time for MFCs with 0.4 wt% Pt/MnO_2 and MnO_2 cathodes. It can be seen that the OCV of the MFC with Pt doped catalyst remained constant even after 14 days of operation, while for the MFC with MnO_2 cathode, the OCV dropped significantly within the same duration of operation. For MnO_2, the OCV initially showed a value of 0.43 V which then dropped to that of around 0.3 V. This decrease is considered as a significant drop. Meanwhile, OCV of Pt/MnO_2 which initially was 0.63 V saw a decrease in trend to around 0.52 V. It was then the OCV increased back to 0.62 V which remained quite constant. The results clearly indicate that the performance of MnO_2 cathode is enhanced due to the Pt doping on MnO_2 as electrocatalyst for ORR.

4.8 Chemical Oxygen Demand (COD) Removal Efficiency

To evaluate the performance of MFCs, its efficiency in treating wastewater is determined. The initial COD of the diluted POME for all sets of MFCs with different catalysts were measured before the commencement of experiment. After 7 days, COD values of the POME treated under MFCs with different catalysts were recorded where each COD removal efficiency was calculated based on equation 3.3. From table 4.5, it can be seen that the COD removal efficiency of 0.4 - 0.8 wt% Pt/MnO_2 based MFCs was slightly higher than that of MnO_2 based MFC.

Table 4-5: COD removal efficiency of catalysts

Catalysts	COD removal efficiency, %
MnO_2	78
0.2 wt% Pt/MnO_2	79
0.4 wt% Pt/MnO_2	84
0.8 wt% Pt/MnO_2	83

5 CONCLUSION AND RECOMMENDATION

5.1 Conclusion

In summary, MnO_2 and Pt/ MnO_2 nanostructured catalysts were successfully synthesized and characterized. The Pt loading and their phases were confirmed by XRD and XPS. FESEM revealed the formation of urchin like structure of MnO_2 which transformed to cocoon type phase after Pt doping. The electrochemical active are was increased with the increase in Pt loading. The ORR activity of the 0.4 wt% Pt/MnO_2 catalyst was increased two times compared to MnO_2 catalysts. The catalysts were used in the cathode of the MFC operated with POME as anode substrate. MFC with Pt/MnO_2 (0.4 wt% Pt) as air cathode catalyst generates a maximum power density of 165 mW/ m^3, which is higher than that of MFC with MnO_2 catalyst (95 mW/m^3). The open circuit voltage (OCV) of the MFC operated with MnO_2 cathode gradually decreased during 14 days of operation, whereas the MFC with Pt/MnO_2 cathode remained almost constant throughout the operation suggesting the higher stability of the Pt/MnO_2 catalyst. In view of the outstanding performance of the Pt/MnO_2 catalyst, it has great promising potential in air cathode MFCs without compromising the lower catalyst cost as aimed.

5.2 Recommendation

Pt/MnO_2 catalyst showed promising results to be used in air cathode microbial fuel cell (MFC). The present work was focused on the preparation, characterization and performance evaluation of the Pt/MnO_2 electrocatalysts in air cathode MFC. Even though anode is usually limiting in MFCs, the study showed that the improved electrocatalyst in cathode can enhance the performance of the MFC. In this context, the following studies should be done in future:

1. Effect of catalyst loading on MFC performance: In this work the catalyst loading was fixed at 1.4 mg/cm^2 which is significantly lower than that reported in literatures.
2. Effect of Pt loading on Brunauer-Emmett-Teller (BET) surface area: The surface area in an important factor for catalyst performance. It should be verified the change in the surface area of MnO_2 after addition of platinum (Pt).

3. Effect of doping method on phase change of MnO_2: An unusual phase change was observed on MnO_2 in this study which was verified by FESEM and XRD analysis. The reason for the phase change needs to be explored in order to improve the doping method.
4. Effect of Pt loading on the particle size: In the present study the particle morphology was studied by FESEM, wherein the Pt size could not be determined. Transmission electron microscopy (TEM) is required to determine the Pt size.
5. Electrochemical impedance spectroscopy (EIS) analysis: The individual anode and cathode potentials as well as the impedance study should be performed to determine the polarization and ohmic losses of the air cathode. The study is important to improve the electrode preparation method and operation of air cathode MFC

REFERENCES

Aelterman, P. (2009). Microbial fuel cells for the treatment of waste streams with energy recovery. Ph.D. Thesis, Gent University, Belgium.

Aelterman, P., Rabaey, K., HaiThePham, B. N., & Verstraete, W. (2006). Continuous electricity generation at high voltages and currents using stacked microbial fuel cells. *Environmental Science and Technology, 40,* 3388-3394.

Ahmad, A. D., Ismail, S., & Bhatia, S. (2003). Water recycling from palm oil mill effluent (POME) using membrane technology. *Desalination, 157,* 87-95.

Aldrovandi, A., Marsili, E., Stante, L., Paganin, P., Tabacchioni, S., & Giordano, A. (2009). Sustainable power production in a membrane-less and mediator-less synthetic wastewater microbial fuel cell. *Bioresource Technology, 100,* 3252-3260.

Allen, R. M., & Bennetto, H. P. (1993). Microbial fuel cells: Electricity production from carbohydrates. *Applied Biochemistry Biotechnology, 39*(2), 27-40.

Angenent, L. T., & Wrenn, B. A. (2008). Optimizing mixed-culture bioprocessing to convert wastes into bioenergy. J. D. Wall, C. S. Harwood, A. Demain (Eds.), Bioenergy, ASM Press, Herndon, VA, USA, 179-194.

Arges, C. G., Ramani, V., & Pintauro, P. N. (2010). Anion exchange membrane. *Electrochemical Society Interface,* 31-35.

Awaludin, Z., Suzuki, M., Masud, J., Okajima, T., & Ohsaka, T. (2011). Enhanced electrocatalysis of oxygen reduction on Pt/TaOx/GC. *The Journal of Physical Chemistry C, 115,* 25557-25567.

Baranitharan, E., Khan, M. R., Prasad, D. M. R., & Salihon, J. (2013). Bioelectricity generation from palm oil mill effluent in microbial fuel cell using polyacrylonitrile carbon felt as electrode. *Water, Air and Soil Pollution, 224,* 1533-1543.

Bashyam, R., & Zelenay, P. (2006). A class of non-precious metal composite catalysts for fuel cells. *Nature, 443,* 63-66.

Bera, P., Priolkar, K. R., Gayen, A., Sarode, P. R., Hegde, M. S., Emura, S., Kumashiro, R., Jayaram, V., & Subbanna, G. N. (2003). Ionic dispersion of Pt over CeO_2 by the combustion method: Structural investigation by XRD, TEM, XPS, and EXAFS. *Chemistry Material, 15,* 2049-2060.

Biffinger, J. C., Ray, R., Little, B., & Ringeisen, B. R. (2007). Diversifying biological fuel cell designs by use of nanoporous filters. *Environmental Science and Technology, 41,* 1444-1449.

Birry, P., Mehta, P., Jaouen, F., Dodelet, J. P., Guiot, S. R., & Tartakovsky, B. (2011). *Electrochimica Acta, 56,* 1505-1511.

Borja, R., Bank, C. J., & Sanchez, E. (1996). Anaerobic treatment of palm oil mill effluent in a two-stage up-flow anaerobic sludge blanket (UASB) system. *Journal of Biotechnology*, *45*, 125-135.

Bond, D. R., Holmes, D. E., Tender, L. M., & Lovley, D. R. (2002). Electrode-reducing microorganisms harvesting energy from marine sediments. *Science, 295*, 483-485.

Chae, K. J., Choi, M., Ajayi, F. F., Park, W., Chang, I. S., & Kim, I. S. (2007). Mass transport through a proton exchange membrane (nafion) in microbial fuel cells. *Energy and Fuels*, *22*, 169-176.

Chae, K. J., Choi, M. J., Lee, J. W., Kim, K. Y., & Kim, I. S. (2009). Effect of different substrates on the performance, bacterial diversity, and bacterial viability in microbial fuel cells. *Bioresource Technology*, *100*, 3518-3525.

Chaudhuri, S. K, & Lovley, D. R. (2003). Electricity generation by direct oxidation of glucose in mediatorless microbial fuel cells. *Nature Biotechnology*, *21*, 1229-1232.

Chen, W. M., Qie, L., Shao, Q. G., Yuan, L. X., Zhang, W. X., & Huang, Y. H. (2012). Controllable synthesis of hollow bipyramid β-MnO_2 and its high electrochemical performance for lithium storage application. *Material Interfaces, 4*, 3047-3053.

Cheng, S., Liu, H., & Logan, B. E. (2006). *Electrochemistry Communications*, *8*, 489-494.

Cheng, F., Su, Y., Liang, J., Tao, Z., & Chen, J. (2010). MnO_2-based nanostructures as catalysts for electrochemical oxygen reduction in alkaline media. *Chemistry of Material*, *22*, 898-905.

Chetty, R., Kundu, S., Xia, W., Bron, M., Schuhmann, W., & Chirila, V. (2009). PtRu nanoparticles supported on nitrogen-doped multiwalled carbon nanotubes as catalyst for methanol electrooxidation. *Electrochimica Acta, 54*, 4208-4215.

Choi, T. H., Won, Y. B, Lee, J. W., Shin, D. W., Lee, Y. M., & Kim, M. (2012). Electrochemical performance of microbial fuel cells based on disulfonatedpoly(aryleneether sulfone) membranes. *Journal of Power Sources, 220*, 269-279.

Chung, K., Fujiki, I., & Okabe, S. (2011). Effect of formation of biofilms and chemical scale on the cathode electrode on the performance of a continuous two-chamber microbial fuel cell. *Bioresource Technology*, *102*, 355-360.

Department of Environment, USA (2011). Renewable energy sources. Retrieved 13 October, 2013 from http://www.ecology.com/2011/09/06/fossil-fuels-renewable-energy-resources/

Feng, Y., Wang, X. Logan, B. E., & Lee, H. (2008). Brewery wastewater treatment using air-cathode microbial fuel cells. *Applied Microbiology Biotechnology*, *78*, 873-880.

Ghangrekar, M., & Shinde, V. (2007). Performance of membraneless microbial fuel cell treating wastewater and effect of electrode distance and area on electricity production. *Bioresource Technology*, *98*, 2879-2885.

Ghasemi, M., Shahgaldi, S., Ismail, M., Yaakob, Z., Daud, W. R. W. (2012). New generation of carbon nanocomposite proton exchange membranes in microbial fuel cell systems. *Chemical Engineering Journal*, *184*, 82-89.

Gong, K. P., Yu, P., Su, L., Xiong, S. X., & Mao, L. Q. (2007). Polymer assisted synthesis of manganese dioxide/carbon nanotube nanocomposite with excellent electrocatalytic activity toward reduction of oxygen. *The Journal of Physical Chemistry C*, *111*, 1882-1887.

Greeman, J., Gálvez, A., Giusti, L., & Ieropoulos, I. (2009). Electricity from landfill leachate using microbial fuel cells: Comparison with a biological aerated filter. *Enzyme and Microbial Technology*, *44*, 112-119.

Habermann, W. & Pommer, E. H. (1991). Biological fuel cells with sulphide storage capacity. *Applied Microbiology Biotechnology*, *35*, 128-133.

Harnisch, F., Wirth, S., & Schröder, U. (2009). Effects of substrate and metabolite cross over on the cathodic oxygen reduction reaction in microbial fuel cells: Platinum vs. iron (II) phthalocyanine based electrodes. *Electrochemistry Communications*, 2253-2256.

Haoyu, E., Cheng, S., Scott, K., & Logan, B. (2007). *Journal of Power Sources*, *171*, 275-281.

He, Z., Wagner, N., Minteer, S. D., & Angenent, L. T. (2006). An upflow microbial fuel cell with an interior cathode: Assessment of the internal resistance by impedance spectroscopy. *Environmental Science and Technology*, *40*, 5212-5217.

Hou, Y., Cheng, Y., Hobson, T., & Liu, J. (2010). *Nano Letters*, *10*, 2727-2733.

Huang, L. P., & Logan, B. E. (2008). Electricity generation and treatment of paper recycling wastewater using a microbial fuel cell. *Applied Microbiology Biotechnology*, *80*, 349-355.

Hull, R. B., Li, L., Xing, Y. C., & Chusuei, C. C. (2006). Pt nanoparticle binding on functionalized multiwalled carbon nanotubes. *Chemistry of Materials*, *18*, 1780-1788.

Ieropoulos, I., Greenman, J., & Melhuish, C. (2010). Improved energy output levels from small-scale microbial fuel cells. *Bioelectrochemistry*, *78*, 44-50.

Ji, E., Moon, H., Piao, J., Ha, P. T., An, J., Kim, D., Woo, J. J., Lee, Y., Moon, S. H., Rittmann, B. E., & Chang, I. S. (2011). Interface resistances of anion exchange membranes in microbial fuel cells with low ionic strength. *Biosensors and Bioelectronics*, *26*(7), 3266-3271.

Jin, B., van Leeuwen, H. J., Patel, B., & Yu, Q. (1998). Utilisation of starch processing wastewater for production of microbial biomass protein and fungal α-amylase by *Aspergillus oryzae*. *Bioresource Technology*, *66*, 201-206.

Kim, K. Y., Chae, K. J., Choi, M. J., Yang, E. T., Hwang, M. H., & Kim, I. S. (2012). High quality effluent and electricity production from non-CEM based flow-through type microbial fuel cell. *Chemical Engineering Journal*, *218*, 19–23.

Kim, J. R., Cheng, S., Oh, S. E., & Logan, B. E. (2007b). Power generation using different cation, anion, and ultrafiltration membranes in microbial fuel cells. *Environmental Science and Technology*, *41*(3), 1004-1009.

Kim, B. H., Park, H. S., Kim, H. J., Kim, G. T., Chang, I. S., Lee, J., & Phung, N. T. (2004). Enrichment of microbial community generating electricity using a fuel cell-type electrochemical cell. *Applied Microbiology Biotechnology*, *63*, 672-681.

Kim, J. R., Premier, G. C., Hawkes, F. R., Dinsdale, R. M., & Guwy, A. J. (2009). Development of a tubular microbial fuel cell (MFC) employing a membrane electrode assembly cathode. *Journal of Power Sources*, *187*, 393-399.

Kjeldsen, P., Barlaz, M. A., Rooker, A. P., Baun, A., Ledin, A., & Christensen, T. H. (2002). Present and long-term composition of MSW landfill leachate: A review. *Critical Reviews in Environmental Science and Technology*, *32*(4), 297-336.

Lee, C. Y., Ho, K. L., Lee, D. J., Su, A., & Chang, J. S. (2012). Electricity harvest from wastewaters using microbial fuel cell with sulfide as sole electron donor. *International Journal of Hydrogen Energy*, *37*, 15787-15791.

Leong, J. X., Daud, W. R. W., Ghasemi, M., Liew, K. B., & Ismail, M. (2013). Ion exchange membranes as separators in microbial fuel cells for bioenergy conversion: A comprehensive review. *Renewable and Sustainable Energy Reviews*, *28*, 575-587.

Lewis, N. S., & Nocera, D. G. (2006). Powering the planet: Chemical challenges in solar energy utilization. *Proceedings of the National Academy of Sciences*, *103*(43), 15729-15735.

Lin, C. S., Khan, M. R., & Lin, S. D. (2006). The preparation of Pt nanoparticles by methanol and citrate. *Journal of Colloid Interface Science*, *299*(2), 678-685.

Liu, L., Li, F. B., Feng, C. H., & Li, Z. X. (2009). Microbial fuel cell with an azo-dye-feeding cathode. *Applied Microbiology and Biotechnology*, *85*, 175-183.

Liu, Z., Liu, J., Zhang, S., & Su, Z. (2009). Study of operational performance and electrical response on mediator-less microbial fuel cells fed with carbon-and-protein rich substrates. *Biochemical Engineering Journal*, *45*, 185-191.

Liu, H., & Logan, B. E. (2004). Electricity generation using an air cathode single chamber microbial fuel cell in the presence and absence of a proton exchange membrane. *Environmental Science and Technology*, *38*, 4040-4046.

Liu, H., Ramnarayanan, R. & Logan, B. E. (2004). Production of electricity during wastewater treatment using a single chamber microbial fuel cell. *Environmental Science and Technology*, *38*(7), 2281-2285.

Logan, B. E. (2008). Microbial fuel cells. Wiley & Sons, Inc., Hoboken, New Jersey.

Logan, B. E., Shaoan, C., & Hong, L. (2006). Increased performance of single chamber microbial fuel cells using an improved cathode structure. *Electrochemistry Communications*, *8*, 489-494.

Lu, M., Kharkwal, S., Ng, H. Y., & Fong, S. Y. L. (2011). Carbon nanotube supported MnO_2 catalysts for oxygen reduction reaction and their applications in microbial fuel cells. *Biosensors and Bioelectronics*, *26*, 4728-4732.

Mauritz, K. A., & Moore, R. B. (2004). State of understanding of Nafion. *Chemical Reviews*, *104*, 4535-4585.

Min, B., Cheng, S., & Logan, B. E. (2005a). Electricity generation using membrane and salt bridge microbial fuel cells. *Water Research*, *39*, 1675-1686.

Min, B., Kim, J. R., Oh, S. E., Regan, J. M., & Logan, B. E. (2005b). Electricity generation from swine waste water using microbial fuel cells. *Water Research*, *39*, 4961-4968.

Min, B., & Logan, B. E. (2004). Continuous electricity generation from domestic waste water and organic substrates in a flat plate microbial fuel cell. *Environmental Science and Technology*, *38*, 5809-5814.

Mohan, S. V., Raghavulu, S. V., & Sarma, P. (2008). Biochemical evaluation of bioelectricity production process from anaerobic wastewater treatment in a single chambered microbial fuel cell (MFC) employing glass wool membrane. *Biosensors and Bioelectronics*, *23*, 1326-1332.

Mo, Y., Liang, P., Huang, X., Wang, H., & Cao, X. (2009). Enhancing the stability of power generation of single-chamber microbial fuel cells using an anion exchange membrane. *Journal of Chemical Technology and Biotechnology*, *84*(12), 1767-1772.

Morris, J. M., Jin, S., Wang, J., Zhu, C., & Urynowicz, M. A. (2007). Lead dioxide as an alternative catalyst to platinum in microbial fuel cells. *Electrochemistry Communications*, *9*(7), 1730-1734.

Oh, S., & Logan, B. E. (2005). Hydrogen and electricity production from a food processing wastewater using fermentation and microbial fuel cell technologies. *Water Research*, *39*, 4673-4682.

Pandey, B., Mishra, V., & Agrawal, S. (2011). Production of bio-electricity during waste-water treatment using a single chamber microbial fuel cell. *International Journal of Engineering, Science and Technology*, *3*, 42-47.

Pandit, S., Ghosh, S., Ghangrekar, M. M., & Das, D. (2012). Performance of an anion exchange membrane in association with cathodic parameters in a dual chamber microbial fuel cell. *International Journal of Hydrogen Energy*, *37*, 9383-9392.

Pant, D., & Adholeya, A. (2007). Biological approaches for treatment of distillery wastewater: A review. *Bioresource Technology*, *98*, 2321-2334.

Pant, D., Bogaert, G. V., Diels, L., & Vanbroekhoven, K. (2010a). A review of the substrates used in microbial fuel cells (MFCs) for sustainable energy production. *Bioresource Technology, 101*, 1533-1543.

Pant, D., Bogaert, G. V., Diels, L., & Vanbroekhoven, K. (2010b). Use of novel permeable membrane and air cathodes in acetate microbial fuel cells. *Electrochimica Acta, 55*, 7710-7716.

Pant, et al., Singh, A., Satyawali, Y., & Gupta, R. K. (2008). Effect of carbon and nitrogen source amendment on synthetic dyes decolourizing efficiency of white-rot fungus, *Phanerochaete chrysosporium*. *Journal of Environmental Biology, 29*(1), 79-84.

Park, D. H., & Zeikus, J. G. (2000). Electricity generation in microbial fuel cells using neutral red as an electronophore. *Applied and Environmental Microbiology*, *66*, 1292-1297.

Pawlak, D. A., Ito, M., Oku, M., Shimamura, K, & Fukuda, T. (2002). Interpretation of XPS O (1s) in mixed oxides proved on mixed perovskite crystals. *The Journal of Physical Chemistry B, 106*, 504-507.

Pham, T. H., Rabaey, K., Aelterman, P., Clauwaert, P., Schamphelaire, L. D., & Boon, N. (2006). Microbial fuel cells in relation to conventional anaerobic digestion technology. *English Life Science, 6*, 285-92.

Potter, M. C. (1911). Electrical effects accompanying the decomposition of organic compounds. *Proceedings of Royal Society of London. Series B, 84*(571), 260-276.

Rabaey, K., Lissens, G., Siciliano, S. D., & Verstraete, W. (2003). A microbial fuel cell capable of converting glucose to electricity at high rate and efficiency. *Biotechnology Letters, 25*, 1531-1535.

Rabaey, K., & Verstraete, W. (2005). Microbial fuel cells: Novel biotechnology for energy generation. *Trends in Biotechnology*, *23*(6), 291-298.

Rittmann, B. E., & McCarty, P. L. (2001). Environmental biotechnology: Principles and applications, McGraw-Hill, Boston.

Santosa, S. J. (2008). Palm oil boom in Indonesia: from plantation to downstream products and biodiesel. *Clean Soil, Air, Water*, 36, 453-465.

Schröder, U. (2007). Anodic electron transfer mechanisms in microbial fuel cells and their energy efficiency. *Physical Chemistry Chemical Physics*, *9*(21), 2619-2629.

Siburian, R., & Nakamura, J. (2012). Formation process of Pt subnano-clusters on graphene nanosheets. *The Journal of Physical Chemistry C, 116*, 22947-22953.

Sleutels, T. H. J. A., Hamelers, H. V. M., Rozendal, R. A., & Buisman, C. J. M. (2009). Ion transport resistance in Microbial Electrolysis Cells with anion and cation

exchange membranes. *International Journal of Hydrogen Energy*, *34*, 3612-3620.

Sun, J., Hu, Y., Bi, Z., & Cao, Y. (2009a). Simultaneous decolorization of azo dye and bioelectricity generation using a microfiltration membrane air-cathode single-chamber microbial fuel cell. *Bioresource Technology*, *100*, 3185-3192.

Sun, J., Hu, Y., Bi, Z., & Cao, Y. (2009b). Improved performance of air-cathode single chamber microbial fuel cell for wastewater treatment using microfiltration membranes and multiple sludge inoculation. *Journal of Power Sources*, *187*, 471-479.

Sun, M., Sheng, G. P., Mu, Z. X., Liu, X. W., Chen, Y. Z., Wang, H. L., & Yu, H. Q. (2009). Manipulating the hydrogen production from acetate in a microbial electrolysis cell-microbial fuel cell-coupled system. *Journal of Power Sources*, *191*, 338-343.

Sun, Y., Wei, J., Liang, P., & Huang, X. (2012). Microbial community analysis in biocathode microbial fuel cells packed with different materials. *AMB Express*, 2, 21.

Suzuki S. (1976). Fuel cells with hydrogen-forming bacteria. *Hospital hygiene, Gesundheitswesen und desinfektion*, 159.

Tang, X., Guo, K., Li, H., Du, Z., & Tian, J. (2010). Microfiltration membrane performance in two-chamber microbial fuel cells. *Biochemical Engineering Journal*, *52*, 194-198.

ter Heijne, A., Hamelers, H. V. M., & Buisman, C. J. N. (2007). *Environmental Science and Technology*, 4130-4134.

Van, T. T. H., Jung, C., & Pang, N. J. (2011). Nanostructured $Ti_{0.7}Mo_{0.3}O_2$ Support enhances electron transfer to Pt: High-performance catalyst for oxygen reduction reaction. *Journal of American Chemical Society*, 11716-11724.

Venkata Mohan, S., Srikanth, S., Veer Raghuvulu, S., Mohanakrishna,G., Kumar, A. K., & Sarma, P. N. (2009). Evaluation of the potential of various aquatic exo-systems in harnessing bioelectricity through benthic fuel cell: Effect of electrode assembly and water characteristics. *Bioresource Technology*, *100*, 2240-2246.

Vijayaraghavan, K.,Ahmad, D., & Lesa, R. (2006). Electrolytic treatment of beer brewery wastewater. *Industrial and Engineering Chemistry Research*, *45*, 6854-6859.

Wang, X., Feng, Y., Ren, N., Wang, H., Lee, H., Li, N., & Zhao, Q. (2009). Accelerated start-up of two-chambered microbial fuel cells: Effect of positive poised potential. *Electrochimica Acta*, *54*, 1109-1114.

Wakisaka, M., Suzuki, H., Mitsui, S., Uchida, H., & Watanabe, M. (2008). Increased oxygen coverage at Pt-Fe alloy cathode for the enhanced oxygen reduction reaction studied by EC-XPS. *The Journal of Physical Chemistry C*, *112*, 2750-2755.

Wen, Q., Wang, S. Y., Yan, J., Cong L. J., Pan, Z. C., Ren, Y. M., & Fan, Z. J. (2012). MnO_2-graphene hybrid as an alternative cathodic catalyst to platinum in microbial fuel cells. *Journal of Power Sources*, *216*, 187-191.

Wen, Q., Wu, Y., Cao, D., Zhao, L., & Sun, Q. (2009). Electricity generation and modelling of microbial fuel cell from continuous beer brewery wastewater. *Bioresource Technology, 100,* 4171-4175.

Wu, T. Y., Mohammad, A. W., Jahim, J. M., & Anuar, N. (2008). A holistic approach to managing palm oil mill effluent (POME): Biotechnolgoical advances in the sustainable reuse of POME. *Biotechnology Advances,* 40-52.

Xia, H., Lai, M. O., & Lu, L. (2010). Nanoflaky MnO_2/carbon nanotube nanocomposites as anode materials for lithium-ion batteries. *Journal of Material Chemistry, 20,* 6896-6902.

Xiang, L., Hub, B. X., Steven, S., Yu, L., & Li, B., K. (2011). Electricity generation in continuous flow microbial fuel cells (MFCs) with manganese dioxide (MnO_2) cathodes. *Biochemical Engineering Journal*, *54,* 10-15.

Xing, P., Robertson, G. P., Guiver, M. D., Mikhailenko, S. D., Wang, K., & Kaliaguine, S. (2004). Synthesis and characterization of sulfonated poly(etheretherketone) for proton exchange membranes. *Journal of Membrane Science, 229,* 95-106.

Yong, C., Chang, L., Feng, L., Hui, C., M. (2005). Preparation of Single-crystal Alpha-MnO_2 Nanorods and Nanoneedles from Aqueous Solution. *Journal of Alloys and Compounds,* 397, 282-285.

Yuan, Y., Ahmed, J., & Kim, S. (2011). *Journal of Power Sources*, 1103-1106.

Yuan, Y., Zhou, S. G., & Zhuang, L. (2010). *Journal of Power Sources*, 3490-3493.

Yu, E. H., Cheng, S., Scott, K., & Logan, B. (2007). Microbial fuel cell performance with non-Pt cathode catalysts. *Journal of Power Sources, 171,* 275-281.

Yu, X. H., He, J. H., Wang, D. H., Hu, Y. C., Tian, H., & He, Z C. (2012). Facile controlled synthesis of Pt/MnO_2 nanostructured catalysts and their catalytic performance for oxidative decomposition of formaldehyde. *The Journal of Physical Chemistry C, 116,* 851-860.

Zhang, F., Cheng, S., Pant, D., Bogaert, G.V., & Logan, B.E. (2009). Power generation using an activated carbon and metal mesh cathode in a microbial fuel cell. *Electrochemistry Communications, 11*(11), 2177-2179.

Zhang, Y. P., Hu, Y. Y., Li, S. Z., Sun, J., & Hou, B. (2011). Manganese dioxide-coated carbon nanotubes as an improved cathodic catalyst for oxygen reduction in a microbial fuel cell. *Journal of Power Sources, 196,* 9284-9289.

Zhang, L. X., Liu, C. S., Zhuang, L., Li, W. S., Zhou, S. G., & Zhang, J. T. (2009). Manganese dioxide as an alternative cathodic catalyst to platinum in microbial fuel cells. *Biosensors and Bioelectronics*, *24*, 2825-2829.

Zhang, J. N., Zhao, Q. L., You, S. J., Jiang, J. Q., & Ren, N. Q. (2008). Continuous electricity production from leachate in a novel upflow air-cathode membrane-free microbial fuel cell. *Water Science and Technology*, *57*(7), 1017-1021.

Zhao, F., Harnisch, F., Schroder, U., Scholz, F., Bogdanoff, P., & Hermann, I. (2006). Challenges and constraints of using oxygen cathodes in microbial fuel cells. *Environmental Science and Technology*, *40*(17), 5193-5199.

Zhao, F., Rahunen, N., Varcoe, J. R., Roberts, A. J., Avignone-Rossa, C., Thumser, A. E., & Slade, R. C. T. (2009). Factors affecting the performance of microbial fuel cells for sulphur pollutants removal, *Biosensors and Bioelectronics*, *24*, 1931-1936.

Zhou, C. M., Wang, H J., Peng, F. L, Yu, J. H., Yang, J. (2009). MnO_2/CNT supported Pt and PtRu nanocatalysts for direct methanol fuel cells. *Langmuir*, *25*, 7711-7717.

Zhu, F., Wang, W., Zhang, X., & Tao, G. (2011). Electricity generation in a membrane-less microbial fuel cell with down-flow feeding onto the cathode. *Bioresource Technology*, *102*, 7324–7328.

APPENDICES

A. Components used in air cathode microbial fuel cell construction

Figure A.1: Carbon brush

Figure A.2: Polyacrynitrile carbon felt (PACF)

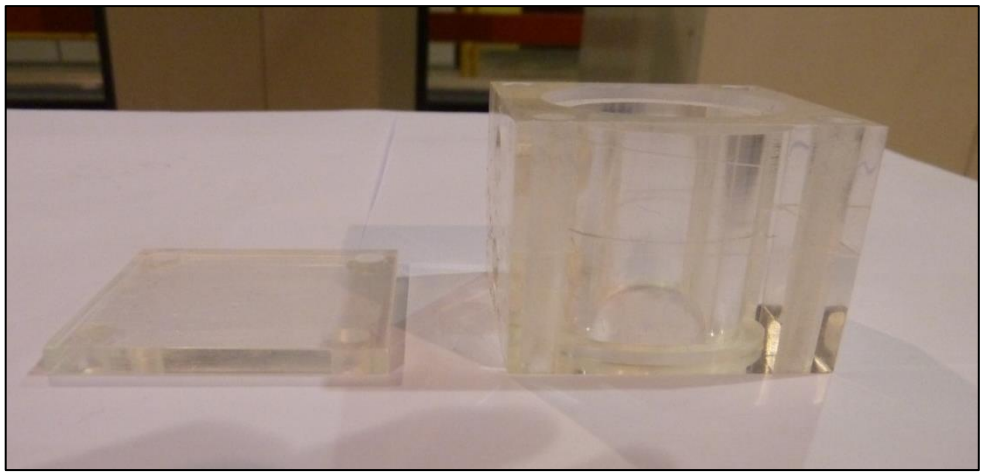

Figure A.3: Plexi cubic glass

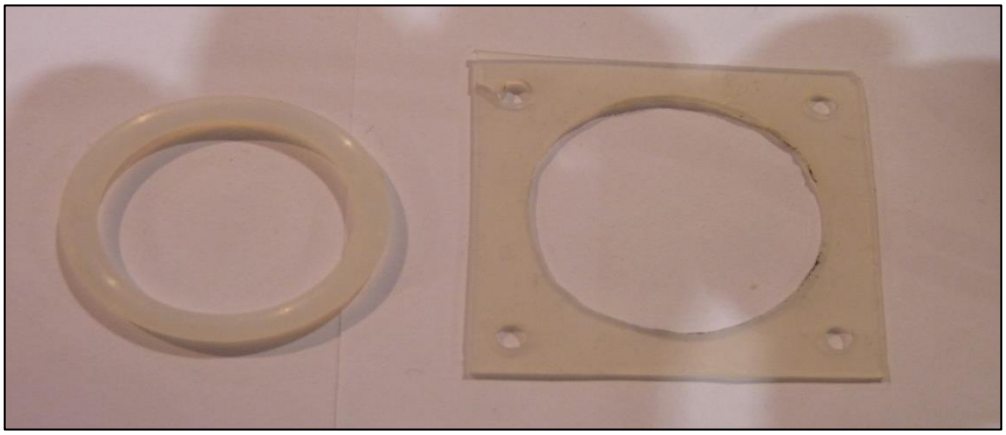

Figure A.4: Ore rings

Figure A.5: Screws

Figure A.6: Titanium wire

Figure A.7: Multimeter

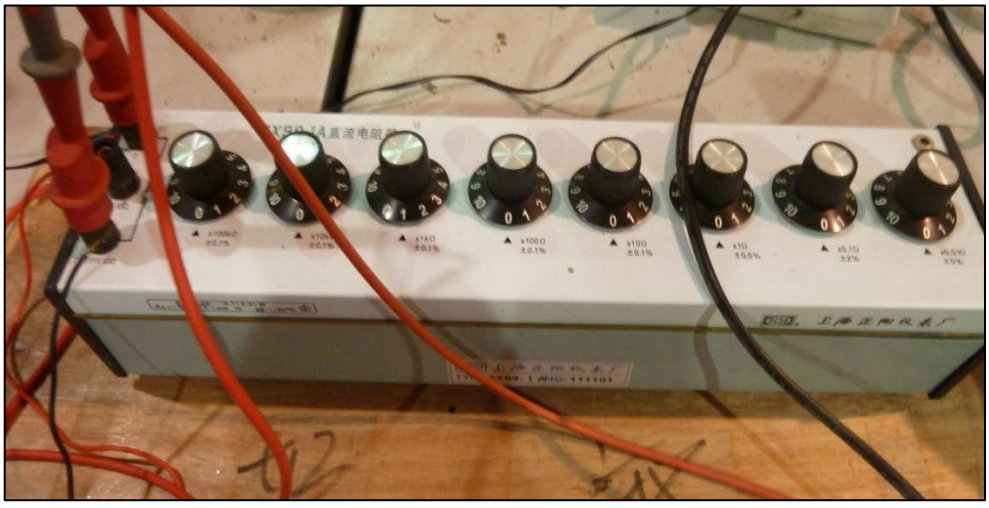

Figure A.8: Resistor

B. Characterization of Pt/MnO_2

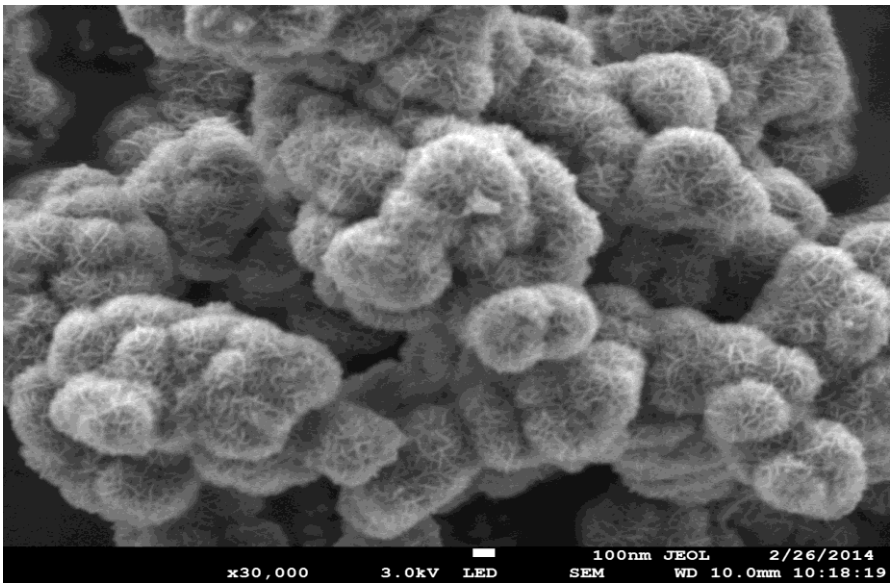

Figure B.1: FESEM of Pt/MnO_2 at 30,000x magnification

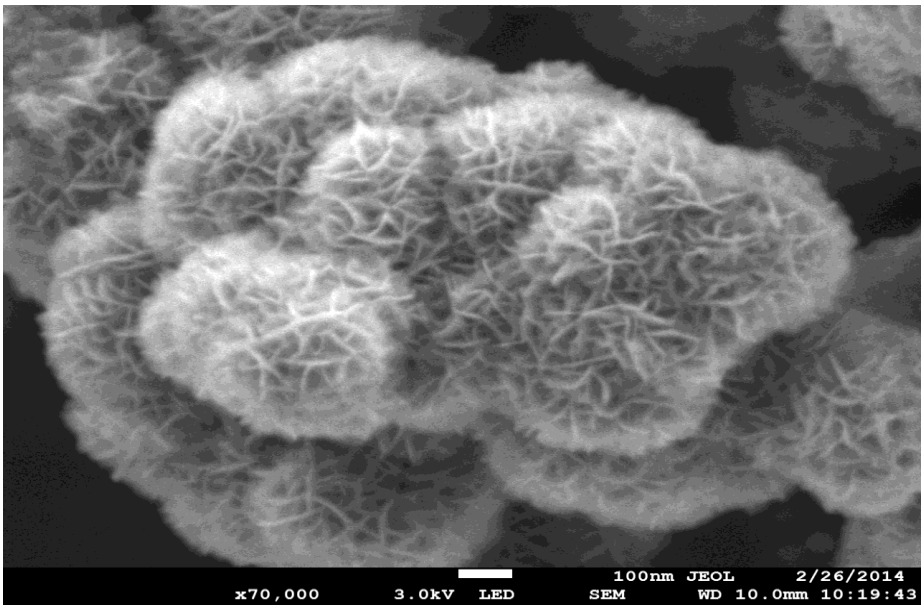

Figure B.2: FESEM of Pt/MnO_2 at 70,000x magnification

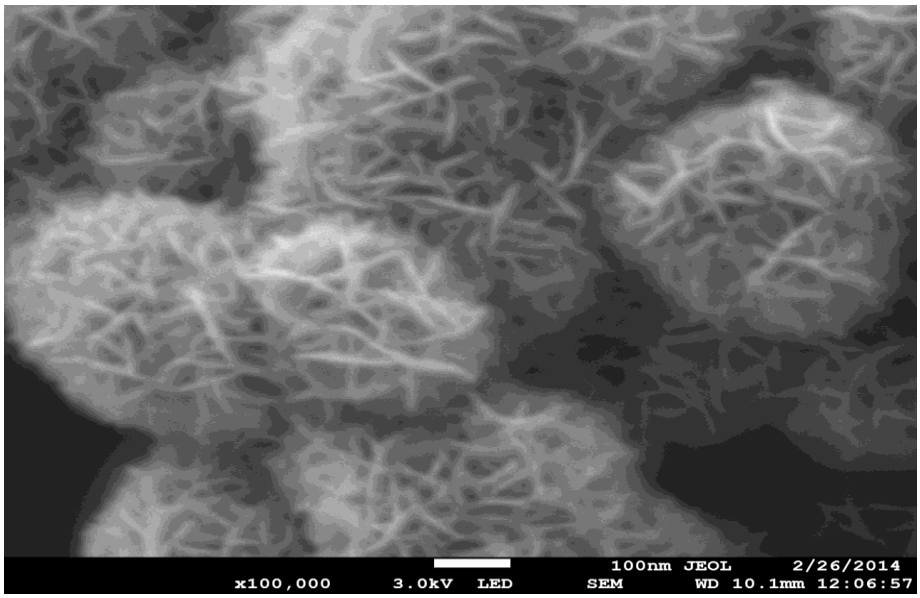

Figure B.3: FESEM of Pt/MnO_2 at 100,000x magnification

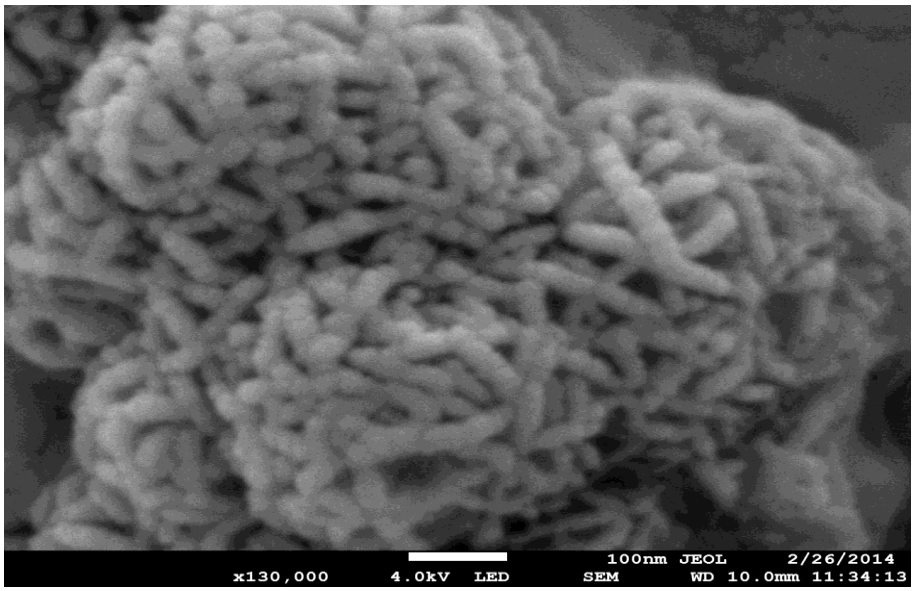

Figure B.4: FESEM of Pt/MnO_2 at 130,000x magnification

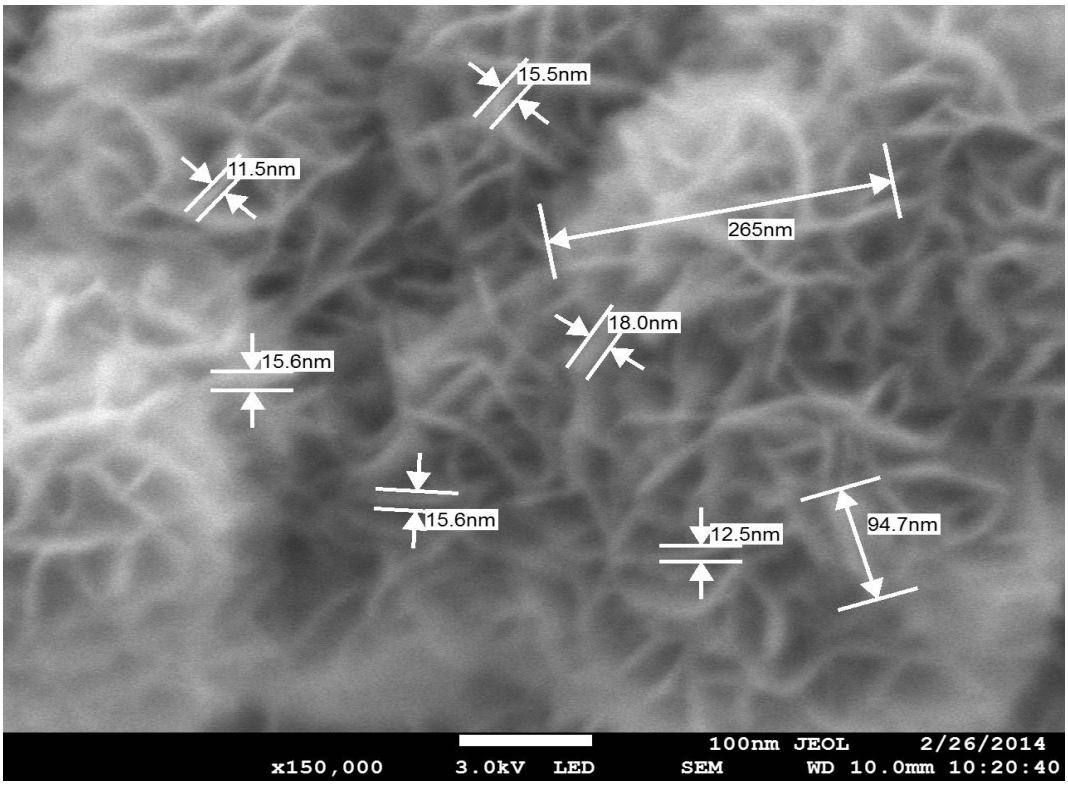

Figure B.5: FESEM of Pt/MnO_2 at 150,000x magnification

C. Power Generation by Air Cathode Microbial Fuel Cell

MnO_2 Catalysts

Table C.1: Polarization data for MnO_2 (1)

Resistance (kΩ)	Voltage (V)	Current (A)	Power (W)
500	0.4100	8.60E-07	3.53E-07
200	0.3789	1.93E-06	7.31E-07
90	0.3252	3.68E-06	1.20E-06
60	0.2965	5.01E-06	1.49E-06
30	0.2345	7.89E-06	1.85E-06
10	0.1324	1.33E-05	1.77E-06
5	0.0769	1.55E-05	1.19E-06
1	0.0186	1.88E-05	3.49E-07
0.5	0.0088	1.75E-05	1.54E-07
0.05	0.0009	1.65E-05	1.49E-08

Table C.2: Polarization data for MnO_2 (2)

Resistance (kΩ)	Voltage (V)	Current (A)	Power (W)
500	3.21E-01	6.80E-07	2.18E-07
200	0.3087	1.58E-06	4.88E-07
90	0.2511	2.84E-06	7.13E-07
60	0.2265	3.83E-06	8.67E-07
30	0.1787	6.02E-06	1.08E-06
10	0.1020	1.03E-05	1.05E-06
5	0.0565	1.14E-05	6.44E-07
1	0.0130	1.30E-05	1.69E-07
0.5	0.0061	1.23E-05	7.49E-08
0.05	0.0006	1.15E-05	6.89E-09

Table C.3: Polarization data for MnO_2 (3)

Resistance (kΩ)	Voltage (V)	Current (A)	Power (W)
500	4.15E-01	8.70E-07	3.61E-07
200	0.3881	1.97E-06	7.65E-07
90	0.3267	3.70E-06	1.21E-06
60	0.2882	4.87E-06	1.40E-06
30	0.2201	7.42E-06	1.63E-06
10	0.1223	1.24E-05	1.51E-06
5	0.0714	1.44E-05	1.03E-06
1	0.0165	1.66E-05	2.73E-07
0.5	0.0076	1.52E-05	1.15E-07
0.05	0.0008	1.53E-05	1.22E-08

Table C.4: Polarization data for MnO_2 (4)

Resistance (kΩ)	Voltage (V)	Current (A)	Power (W)
500	3.54E-01	7.50E-07	2.66E-07
200	0.3331	1.70E-06	5.66E-07
90	0.2761	3.13E-06	8.64E-07
60	0.2482	4.20E-06	1.04E-06
30	0.1886	6.38E-06	1.20E-06
10	0.0962	9.68E-06	9.31E-07
5	0.0554	1.12E-05	6.19E-07
1	0.0123	1.23E-05	1.51E-07
0.5	0.0051	1.00E-05	5.12E-08
0.05	0.0005	9.63E-06	4.82E-09

0.2 wt% Pt/MnO_2 Catalysts

Table C.5: Polarization data for 0.2 wt% Pt/MnO_2 (1)

Resistance (kΩ)	Voltage (V)	Current (A)	Power (W)
500	0.2560	5.40E-07	1.38E-07
200	0.2305	1.18E-06	2.72E-07
90	0.1915	2.17E-06	4.16E-07
60	0.1640	2.77E-06	4.54E-07
30	0.1243	4.19E-06	5.21E-07
10	0.0797	7.91E-06	6.30E-07
5	0.0456	9.18E-06	4.19E-07
1	0.0123	1.22E-05	1.50E-07
0.5	0.0056	1.10E-05	6.16E-08
0.05	0.0006	1.09E-05	6.55E-09

Table C.6: Polarization data for 0.2 wt% Pt/MnO_2 (2)

Resistance (kΩ)	Voltage (V)	Current (A)	Power (W)
500	0.1244	2.70E-07	3.36E-08
200	0.1131	5.80E-07	6.56E-08
90	0.1027	1.17E-06	1.20E-07
60	0.0882	2.32E-06	2.05E-07
30	0.0685	2.32E-06	1.59E-07
10	0.0407	4.11E-06	1.67E-07
5	0.0265	5.35E-06	1.42E-07
1	0.0076	7.61E-06	5.78E-08
0.5	0.0043	8.69E-06	3.74E-08
0.05	0.0006	1.05E-05	6.30E-09

0.4 wt% Pt/MnO_2 Catalyst

Table C.7: Polarization data for 0.4 wt% Pt/MnO_2 (1)

Resistance (kΩ)	Voltage (V)	Current (A)	Power (W)
500	0.5860	1.22E-06	7.15E-07
200	0.5440	2.77E-06	1.51E-06
90	0.4575	5.17E-06	2.37E-06
60	0.4025	6.79E-06	2.73E-06
30	0.3125	1.05E-05	3.28E-06
10	0.1665	1.67E-05	2.79E-06
9	0.1438	1.61E-05	2.32E-06
5	0.0907	1.82E-05	1.65E-06
1	0.0220	2.21E-05	4.86E-07
0.5	0.0108	2.15E-05	2.32E-07
0.05	0.0011	2.34E-05	2.57E-08

0.8 wt% Pt/MnO_2 Catalysts

Table C.8: Polarization data for 0.8 wt% Pt/MnO_2 (1)

Resistance (kΩ)	Voltage (V)	Current (A)	Power (W)
500	0.4851	1.02E-06	4.95E-07
200	0.4425	2.25E-06	9.96E-07
90	0.3636	4.11E-06	1.49E-06
60	0.3270	5.53E-06	1.81E-06
30	0.2551	8.58E-06	2.19E-06
10	0.1339	1.35E-05	1.80E-06
5	0.0757	1.52E-05	1.15E-06
1	0.0190	1.91E-05	3.62E-07
0.5	0.0091	1.83E-05	1.67E-07
0.05	0.0010	1.89E-05	1.89E-08

Table C.9: Polarization data for 0.8 wt% Pt/MnO_2 (2)

Resistance (kΩ)	Voltage (V)	Current (A)	Power (W)
500	0.5247	1.10E-06	5.77E-07
200	0.4736	2.42E-06	1.15E-06
90	0.4145	4.68E-06	1.94E-06
60	0.3545	5.98E-06	2.12E-06
30	0.2694	9.07E-06	2.44E-06
10	0.1438	1.45E-05	2.08E-06
5	0.0857	1.73E-05	1.48E-06
1	0.0211	2.12E-05	4.48E-07
0.5	0.0108	2.17E-05	2.34E-07
0.05	0.0011	2.19E-05	2.41E-08

Table C.10: Polarization data for 0.8 wt% Pt/MnO_2 (3)

Resistance (kΩ)	Voltage (V)	Current (A)	Power (W)
500	0.4970	1.03E-06	5.12E-07
200	0.4479	2.28E-06	1.02E-06
90	0.3822	4.31E-06	1.65E-06
60	0.3311	5.61E-06	1.86E-06
30	0.2471	8.33E-06	2.06E-06
10	0.1314	1.32E-05	1.74E-06
5	0.0760	1.53E-05	1.17E-06
1	0.0188	1.89E-05	3.56E-07
0.5	0.0086	1.72E-05	1.48E-07
0.05	0.0009	1.67E-05	1.50E-08